AOARD final report

- **Title of Proposed Research :**

Vertical alignment of single-walled carbon nanotubes on nanostructure fabricated by atomic force microscope

- **Name of Principal Investigator :**

  Haiwon Lee

- **Affiliation of Researcher(s) :**

  Hanyang University

- **Address of Researcher(s) :**

  Department of Chemistry, Hanyang University, 17 Haengdang-dong, Seongdong-gu, Seoul 133-791, Korea
  Phone: +82-2-2220-0945
  FAX: +82-2-2296-0287

- Past AOARD or US government support

Report Documentation Page

Form Approved
OMB No. 0704-0188

1. REPORT DATE	2. REPORT TYPE	3. DATES COVERED
16 FEB 2007		

4. TITLE AND SUBTITLE	5a. CONTRACT NUMBER
Vertical alignment of single-walled carbon nanotubes on nanostructure fabricated by atomic force microscope	5b. GRANT NUMBER
	5c. PROGRAM ELEMENT NUMBER
6. AUTHOR(S)	5d. PROJECT NUMBER
Haiwon Lee	5e. TASK NUMBER
	5f. WORK UNIT NUMBER
7. PERFORMING ORGANIZATION NAME(S) AND ADDRESS(ES)	8. PERFORMING ORGANIZATION REPORT NUMBER
Hanyang University,Haengdang-dong, ,Seongdong-gu,Seoul 133-791 KOREA,KE,133-791	**AOARD-044053**
9. SPONSORING/MONITORING AGENCY NAME(S) AND ADDRESS(ES)	10. SPONSOR/MONITOR'S ACRONYM(S)
	11. SPONSOR/MONITOR'S REPORT NUMBER(S)

12. DISTRIBUTION/AVAILABILITY STATEMENT

Approved for public release; distribution unlimited.

13. SUPPLEMENTARY NOTES

14. ABSTRACT

Our work has been concentrated on both chemical attachments of functionalized carbonnanotubes (CNTs) and their alignments through chemical, electrical and optical manipulation on templates such as Si-wafer and gold, on which nanostructures can be formed by novellithographic techniques of atomic force microscope (AFM) anodic oxidation lithography or nanosphere lithography. As-grown CNTs were modified with functional groups like carboxylic acid, acid chloride and alkyl thiol groups to chemically bond CNTs to templates. The chemical bonding of functionalized CNTs on conducting templates was also performed by applying a direct current (DC) field to CNT suspension, resulting in the formation of uniform CNT films. Ultrasonic treatment allowed the electrodeposited CNTs to be aligned normal to the electrodes. In addition, the selective attachment of CNTs on templates was conducted by applying the lithographic techniques. A promising approach to manipulating CNTs was demonstrated using a linear polarized infrared optical trapping system. Various analytical methods such as AFM, TEM SEM, Raman, FT-IR, and field emission measurement enabled the characterization of the CNTs.

15. SUBJECT TERMS

16. SECURITY CLASSIFICATION OF:			17. LIMITATION OF ABSTRACT	18. NUMBER OF PAGES	19a. NAME OF RESPONSIBLE PERSON
a. REPORT	b. ABSTRACT	c. THIS PAGE			
unclassified	**unclassified**	**unclassified**		**50**	

Abstract

Our work has been concentrated on both chemical attachments of functionalized carbon nanotubes (CNTs) and their alignments through chemical, electrical and optical manipulation on templates such as Si-wafer and gold, on which nanostructures can be formed by novel lithographic techniques of atomic force microscope (AFM) anodic oxidation lithography or nanosphere lithography. As-grown CNTs were modified with functional groups like carboxylic acid, acid chloride and alkyl thiol groups to chemically bond CNTs to templates. The chemical bonding of functionalized CNTs on conducting templates was also performed by applying a direct current (DC) field to CNT suspension, resulting in the formation of uniform CNT films. Ultrasonic treatment allowed the electrodeposited CNTs to be aligned normal to the electrodes. In addition, the selective attachment of CNTs on templates was conducted by applying the lithographic techniques. A promising approach to manipulating CNTs was demonstrated using a linear polarized infrared optical trapping system. Various analytical methods such as AFM, TEM, SEM, Raman, FT-IR, and field emission measurement enabled the characterization of the CNTs.

1. Introduction

While it has long been known that carbon fibres can be produced with a carbon arc, and patents were issued for the process, it was not until 1991 that Sumio Iijima, a researcher with the NEC Corporation in Japan, observed that these fibres were hollow. Carbon nanotubes (CNTs) are tubular carbon molecules with properties that make them potentially useful in extremely small-scale applications. They exhibit unusual strength and unique electrical properties. Accordingly, the number of both specialized and large-scale applications is growing constantly, including their use as conductive and high-strength composites, energy storage and energy conversion devices, sensors, field emission displays and radiation sources, hydrogen storage media, nanometer-sized semiconductor devices, probes, interconnects, etc. Nanotubes can be opened and filled with materials such as biological molecules, raising the possibility of applications in biotechnology. They can be used to dissipate heat from tiny computer chips. The strength and flexibility of carbon nanotubes makes them of potential use in controlling other nanoscale structures, which suggests they will have an important role in nanotechnology engineering. With only a few nanometers in diameter, yet (presently) up to a millimeter long, the length-to-width aspect ratio is extremely high. Atomic force microscopy (AFM) is now widely used and has the capability of working at length scales as small as a single atom. The AFM resolution depends highly on the curvature of AFM tip. To overcome broad tip curvature carbon nanotubes are used as a probe called ‘CNT tips’ which are usually applied for characterization of large and complex bio molecules with high resolution or AFM lithography to fabricate patterns with high aspect ratios.

To apply such SWNTs to various technologies, well-aligned carbon nanotubes are desirable. To date, there have been a number of efforts for aligning carbon nanotubes with direct growth methods like chemical vapor deposition (CVD), which generally works in high-temperature circumstances. There have been great challenges to finding an effective way to organize and/or to manipulate as-grown tangled nanotubes into well-ordered arrays in mild conditions. Chemical processing of as-grown CNTs has allowed CNTs to be controlled in length, purified, modified

with functional groups, dispersed in desired solvents and eventually aligned on substrates. Moreover, various methods for aligning chemically functionalized CNTs, such as self-assembly methods, hydrophilic/hydrophobic interactions and electrochemistry, have also been introduced because of their simplicity at ambient temperature and their applicability to relatively large areas. Using these controllable processes, horizontally aligned and micropatterned carbon nanotubes have been performed to apply carbon nanotubes as an active component to carbon nanotube-based devices. Vertically aligned and micropatterned carbon nanotubes, however, have been poorly studied especially by post-synthesis treatments rather than by the direct growth like chemical vapor deposition (CVD). For instance, functionalized CNTs have been believed to be vertically assembled on modified substrates analogous to the self-assembly processes of active surfactant molecules such as alkanethiols and organosilicons. Even though the shapes of CNTs, which usually disperse as bundles in solution, resemble the long-chain molecules available for ordering into self-assembled monolayers, it would be difficult for CNT bundles to be spontaneously aligned to the surface normal direction like surfactant molecules due to their enormous, irregular size in suspension and low density of CNTs on modified surfaces. Recently, a direct current (DC) electrodeposition method has been applied to forming CNT films efficiently on substrates. Applying the electric field as an external force to CNT suspensions made it possible to provide high surface coverages and short assembling times. The highly densified CNT films produced by electrodeposition, however, are randomly aligned and also pressured by strong electric field, resulting in almost flat CNT films accumulated with high randomness of orientation which limits their applications. Here, we report the chemical functionalization of CNTs, their attachment with controllable processes, and vertical alignments of CNT films formed by electrodeposition.

2. Approach and results

2-1. Functionalization of CNTs and chemical attachments

The purified single-walled carbon nanotubes (HiPCO SWNTs) were purchased from Carbon Nanotechnologies Inc. The carboxyl groups-terminated SWNTs (SWNT-COOH) were prepared by shortening and etching processes using ultrasonification in mixed acids of sulfuric acid and nitric acid (3:1). Scheme 1 shows the path ways of reaction to functionalize SWNTs and to attach the SWNTs on modified templates. The carboxyl group of shortened SWNTs were modified with $SOCl_2$ and cysteamine to change the functional group from carboxyl group to acyl chloride (-COCl) and thiol (-$CONH(CH_2)_2SH$) group, respectively. The chemically functionalized SWNTs were confirmed by FT-IR (Bruker, USA). Fig. 1 shows the FT-IR spectra of (a) SWNT-COOH, (b) SWNT-COCl, and (c) SWNT-SH. The carbonyl (C=O) band of SWNT-COOH and SWNT-COCl were appeared in 1720 cm^{-1} and 1760 cm^{-1}, respectively. Because of existence of the chlorine in the SWNT-COCl that has higher electronegativity compared to oxygen in the SWNT-COOH, the carbonyl band sifted to 1760 cm^{-1}. And the carbonyl (C=O) and amide (N-H) bands of SWNT-$CONH(CH_2)_2SH$ were appeared in 1720 cm^{-1} and 1550 cm^{-1}, respectively.

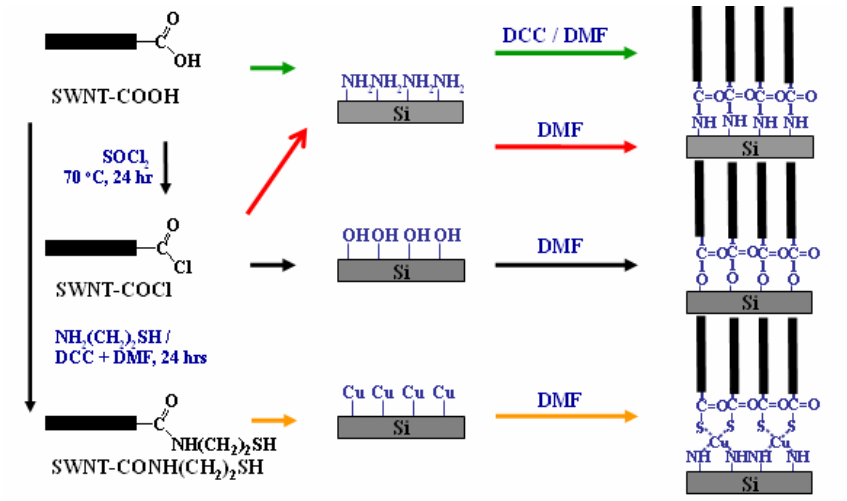

Scheme 1. Schematic of attachments of chemically functionalized SWNTs on modified templates.

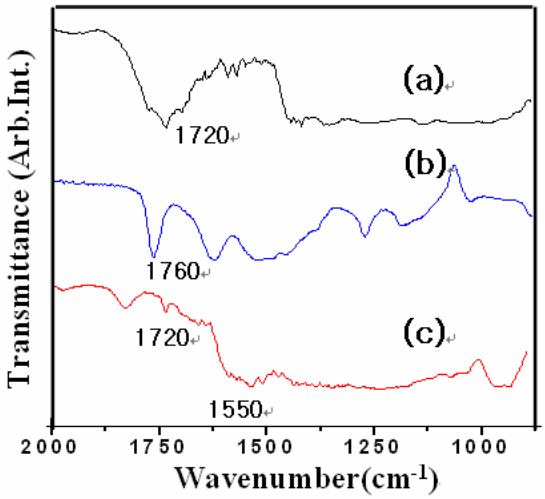

Figure 1. The FT-IR spectra of (a) SWNT-COOH, (b) SWNT-COCl, and (c) SWNT-$CONH(CH_2)_2SH$.

The SWNTs-COCl were reacted with hydroxyl groups and 3-(aminopropyl) triethoxylmethyl-silane (APS) self-assembled on substrates. Also, the variations in thickness of functionalized templates were characterized using an ellipsometer (Rudolph Auto EL2). The amine modified template was reacted with the SWNT-COOH and dicyclohexylcarbodiimide (DCC) as a condensation agent. And SWNT-$CONH(CH_2)_2SH$ was reacted with (3-(2-aminoethyl)amino-propyl) trimethoxysilane (AEAPS) monolayers and copper(Ⅱ) nitrate ($Cu(NO_3)_2$). For selective attachment of thiolated SWNTs, octadecyltrichlorosilane (OTS) was self-assembled on the silicon oxide substrate by dipping Si wafer. Because the thiolated SWNTs can not bind methyl group, the OTS modified surface was used as a barrier. And the thiolated SWNTs were bound on the copper-amine complex by coordination reaction. The SWNTs suspension in

dimethylformamide reacted for 12 hrs at room temperature. After reaction, the templates were rinsed with DMF under sonication followed by drying under a stream of nitrogen. Non-contact mode AFM (XE-100, PSIA Inc.) was exploited to characterize the surface morphologies. The methodology utilizes the strong interaction between the functional groups on templates and the functional groups of SWNTs. The APS and AEAPS are used to react with surface hydroxyl groups. This will result in a surface covered with amine groups. Fig. 2 shows AFM images of attached SWNTs on chemically modified surfaces. Fig. 2 (b) shows the most densely attached SWNTs among any other path ways. Because this reaction is easier than the attachment of SWNT-COOH and SWNT- $CONH(CH_2)_2SH$ (Fig. 2a and d) that needs another materials, such as condensation agent and copper(Ⅱ) nitrate, to be attached onto the amine group modified templates. Those additional thiolated SWNTs were reacted with NH_2-Cu complex surface that makes complicated reaction process. Though thiolated SWNTs can be attached to gold surface, the functionalized SWNTs attached on Si substrate to compare the reactivity of the SWNTs. In comparison of Fig. 2 (b) and (c), the hydrogen of hydroxyl groups can not be easily detached compared with the hydrogen of amine group ($–NH_2$). However, the chloride ion of SWNT-COCl is a good leaving group and hydrogen of $–NH_2$ can be easily dehydrogenated. As a result, the high degree of attachment with SWNTs can be accomplished by chemical reaction of the functionalized SWNT-COCl with on amine group modified template.

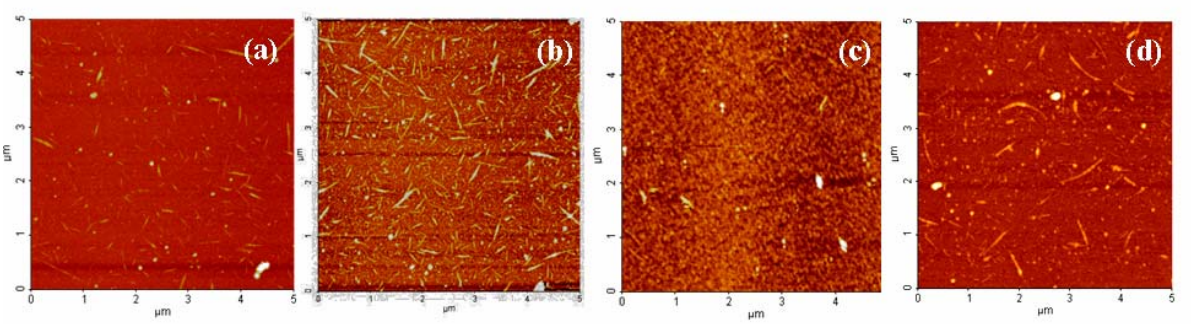

Figure 2. AFM images of attached SWNTs on modified templates: (a) SWNT-COOH and (b) SWNT-COCl on amine group modified template. (c) SWNT-COCl on hydroxyl modified template and (d) SWNT-$CONH(CH_2)_2SH$ on amine-copper group modified template.

Chemical binding of nanospheres-NH_2 with SWNTs-COCl was conducted to fabricate effective nanostructures. Figure 3 shows wonderful images of nanospheres selectively combined with a bunch of SWNTs. In the cutting process of SWNTs using oxidizing acid, many defects are produced on the side wall of SWNTs, analogous to both ends of SWNTs. These defects also are terminated with –COOH groups, which can be active sites to react with substitutes. To date, it has been focused on improving physical, chemical and electrical properties of SWNTs through chemical attachments of useful substances on the side defects of SWNTs from many research groups. The alignment of carbon nanotubes also has been critical issue to apply them to the area of molecular electronics, field emission display, etc. As shown in Figure 3, the PS nanospheres attached on the SWNTs would not seem to change much the properties of SWNTs and also to improve the alignment greatly. However, it is very important to selectively attach nanospheres onto SWNTs because these basic structures have quite a possibility to be used to make a practical application of SWNTs.

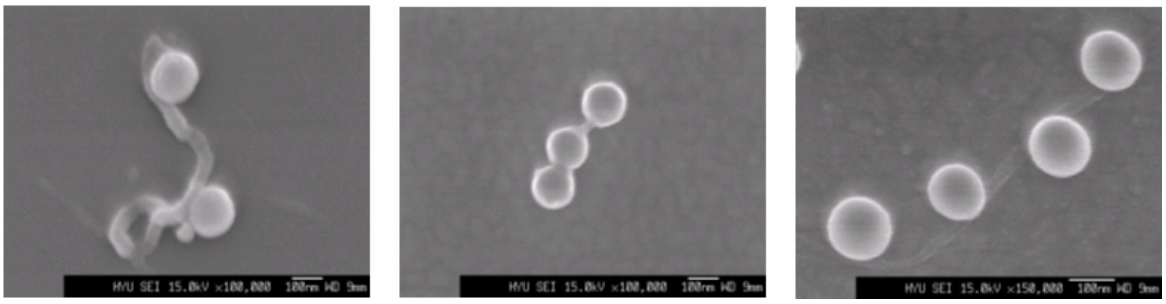

Figure 3 Scanning Electron Microscope (SEM) images of 190 nm of PS nanospheres chemically attached on the SWNTs.

Based on chemical reactions of the modified SWNTs with functionalized surfaces, we tried selective attachments of SWNTs on patterned surfaces as shown in Figure 4(a). We chose self-assembled monolayer (SAM) of hexamethyldisilane (HMDS) as a resist whose surface was covered by methyl groups (-CH_3). Since there is no reaction between chemically modified SWNTs and CH_3 groups, SWNT-COCl will be reacted only with the patterned area containing –OH groups. In AFM anodization lithography, patterning was achieved by the growth of silicon oxide which contained –OH groups as shown in Figure 4(b, top). As a result, the patterned area is covered by –OH group while unpatterned area is covered by –CH_3 group. Figure 4(b, bottom) shows selectively attached SWNTs on the protruded SiO_2 region. The height of attached SWNTs on patterned surfaces ranges from 6 nm to 18 nm which are too low for these values to be regarded as those of SWNTs. In fact, the materials attached on line patterns are a kind of carbon which can be clearly confirmed by phase mode AFM. Moreover, in Figure 4(b, bottom), what it was selectively attached means that the chemical reaction occurred only on patterned area. Hence, it can be suggested that line patterns containing –OH groups react rapidly with very thin SWNTs-COCl separated from the aggregates as well as carbon particles also modified with –COCl since their mobility is better than bulkily-aggregated SWNTs in solution. The similar selective attachment of SWNTs was observed on the various types of patterns.

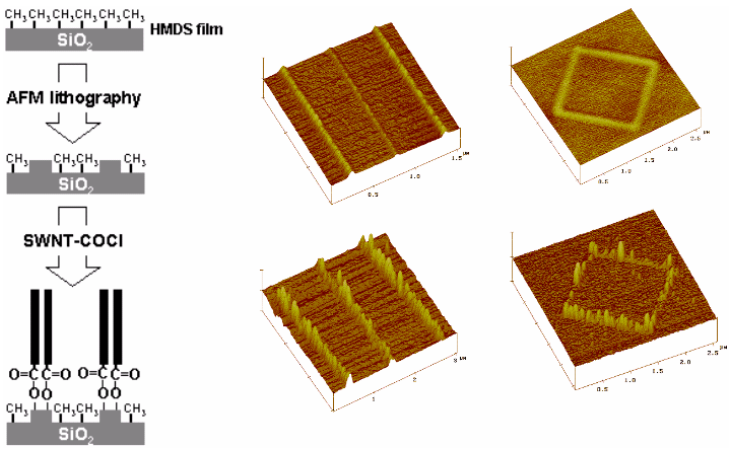

(a) (b)

Figure 4 (a) Schematic for selectively attachments of SWNTs on prepatterned surfaces, representative tapping mode AFM images of patterned HAMD SAM (b, top) before and (b, bottom) after reaction with SWNTs.

2-2. Optical trapping of CNTs

Another approach to manipulating CNTs was demonstrated using a linear polarized infrared optical trapping system. Optical tweezers is a powerful tool for processing nano-size objects, and this technique can also be used to trap and manipulate SWNTs. But in previous reports, only trapping of the CNTs with optical tweezers was given, and manipulation of SWNT bundles vertically and spinning MWNTs vertically have not yet been reported. To construct 2-D or 3-D nanostructures, more exact control of the trapping is essential. To explore how to trap and manipulate CNTs more precisely, an infrared optical tweezers system is used to manipulate various CNTs of different fabrication methods, chemical modifications, and sizes. The linearly polarized laser diode (SDL-5432H1, λ=834 nm) is used as the trapping light source. The beam expander is composed of two convex lenses. The 120 mW laser beam is strongly focused by an objective lens (Zeith, 100×, oil immersion type, N.A. =1.25, the radius of its back aperture: 2.5 mm) and forms a single-beam optical trap with a diameter less than 1 μm. The sample stage is maintained with a computer-controlled motorized controller (Newport, M-UTM25PP.1, resolution 0.1 μm). The trapping process can be recorded with a CCD camera from linear or circular polarization. A chamber composed of cover- and slide-glass is used to seal a drop of the CNT aqueous solution.

Naturally the short CNT (SWNT and MWNT) bundles have lengths of a few hundred nanometers to 1 μm and diameters of about 20 nm after being cut in mixed acid. All the CNTs used in this study are referred to as CNT bundle, which consist of many short CNTs held together by molecular forces. Figures 5(a) and 5(b) show that one CNT bundle can be trapped vertically and horizontally, respectively. In vertical trapping, the CNT bundle is aligned along the propagation direction of the laser beam while the CNT bundle is aligned along the transverse direction of the laser beam in horizontal trapping. The vertically and horizontally trapped CNTs can be manipulated into any specific position with the optical trap. Vertical trapping was confirmed by a point image because the CCD camera captured top view images. Shorter CNTs are much easier to trap vertically if the focused laser beam is applied to the end of the CNT. Optical tweezers cannot easily trap longer CNTs vertically. If the length of the CNTs is shorter than 10 μm, they can be trapped vertically by decreasing the distance between the substrate and the trapped position just after picking one end. If the distance between the substrate and the trapped position is increased, vertical trapping cannot be achieved. In other words, horizontal trapping of one CNT bundle can be switched to vertical trapping by adjusting the trapping depth (the distance between the cover glass and the trapping position). In our experiment, an oil immersion lens was used to focus the beam. When the trapping depth is zero, the laser intensity is concentrated near the beam focus symmetrically, where the trapping force would trap a partial position of the CNT bundle but strong enough to hold the whole CNTs. When the trapping depth is increased, the convergence angle decreases and the beam intensity is distributed more along the central axis of the beam before the focus point, which means that the optical trapping force is also distributed along the central axis. This can provide the possibility for long CNTs to be trapped vertically. Small CNT bundles can be trapped collectively as shown in Figure 5(c). These trapped bundles of CNTs can also be manipulated along the transverse direction by dragging them with the laser beam. Such collective trapping may be due to the induced polarization of originally trapped central CNTs when the dipole moments of the polarized CNTs attract nearby smaller CNTs. The optical trap can manipulate CNTs, so it could also be used to construct special CNTs structures. For example, CNTs could be fixed onto the glass vertically or horizontally. Figure 5(d) shows that by trapping and dragging the CNTs horizontally, two letters

were constructed on the glass substrate. Two crossing CNT bundles built the letter "**X**". The end of one CNT bundle was bound to the side-wall of another CNT bundle to make the letter "**Y**". Similarly, by manipulating CNTs vertically, bundles can be fixed onto the glass. In Figure 5(e), one end of the CNTs has been fixed onto the glass marked by a small white circle. The other end of the CNTs is swaying freely in the solution. The position of the optical trap is marked by a big white circle. This manipulation can also be done on ITO glass, which can be used to assemble some CNT-based electronic devices. Small CNTs with lengths of a few hundred nanometers are rather difficult to fix onto the glass. We fixed the CNTs functionalized with groups of –COCl and PS (polystyrene) particles modified with an amine group together. The mixture was placed at room temperature for 24 hours before the trapping experiment, until the ends and sidewalls of most CNTs in the solution were attached to PS particles. Figure 5(f) is a CCD image of a dot array consisting of CNTs and PS particles. The size of the dot was controlled by the application time of the optical tweezers. The large dots on the left of the array were made by a longer application time. The inset SEM image of one dot in Figure 5(f) shows many PS particles aggregated with CNTs in the optical trap. In this process, the CNTs played an important role as an adhesive to initiate the formation of the large clusters.

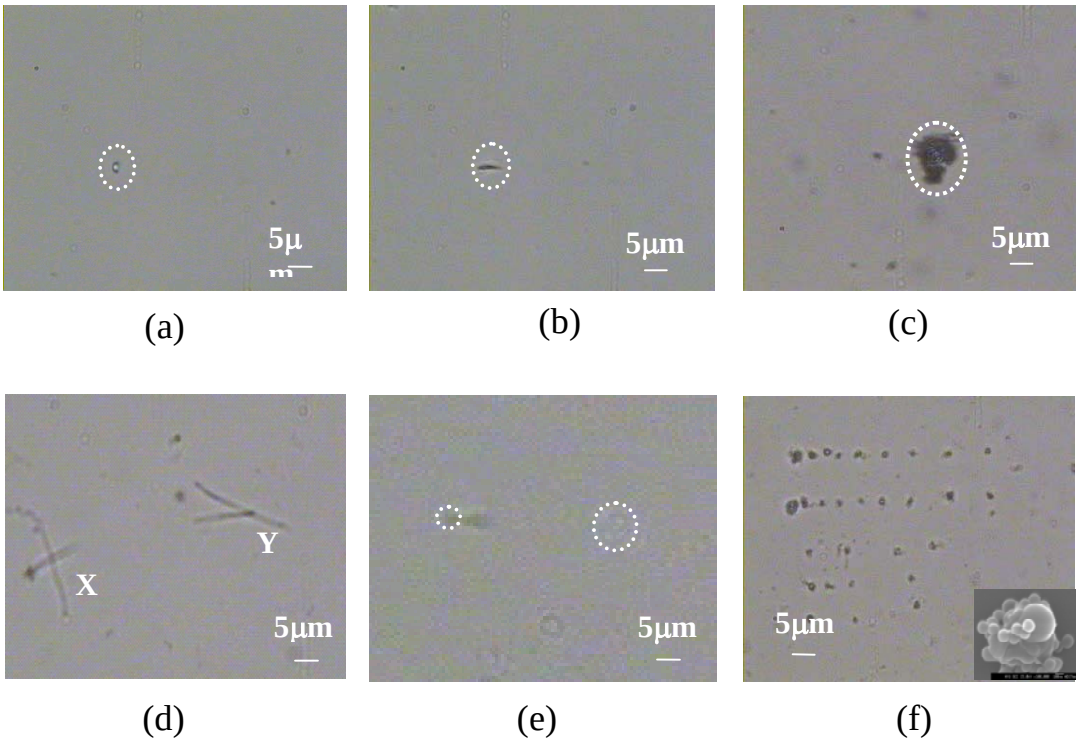

Figure 5. CCD images of optical manipulation of the CNT bundle: (a) Vertical trapping, (b) horizontal trapping, (c) collective trapping of CNTs in highly concentrated CNT solution, (d) constructing CNT letters horizontally, (e) vertical fixing of a CNT bundle, (f) constructing a CNT/PS array, and inset is a SEM image of one CNT/PS dot.

2-3. Electrodeposition of CNTs and vertical alignment

The acid chloride-functionalized SWNTs were attached to chemically modified substrates using electrodeposition method. Scheme 2 shows a simple drawing of electrophoretic deposition

of a bundle of SWNTs-COCl on NH_2 group-terminated gold substrate and electrophoretic cells containing SWNTs suspension before and after applying a dc field. Once the electric field was applied to the suspension in the cell, SWNTs migrated along with the convectional flowing of the suspension in the middle space between electrodes.

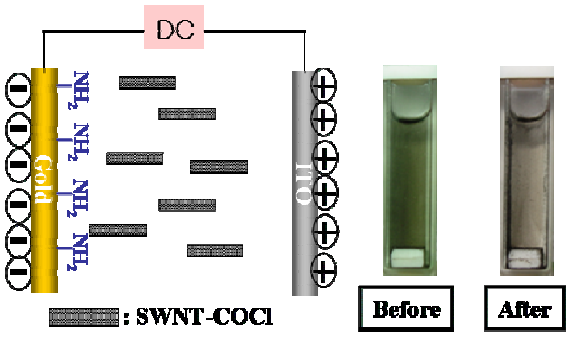

Scheme 2. Simple drawing of the electrophoretic deposition of SWNTs-COCl on gold electrode functionalized with SAM terminating in amine group using a dc field and the electrophoretic cells containing SWNT suspension before and after applying a dc field.

The high-speed migration of SWNTs was observed near to both electrodes where the electric field is very strong. After a few minutes, the black suspension became transparent due to the deposition of SWNTs on both electrodes. While the robust film of SWNTs was formed on the cathode during applying a voltage, the assembled bundles of SWNTs, which were aligned parallel to the direction of electric field, were physically deposited on the anode without strong adhesion. Rinsing the anode with DMF after completing the electrophoretic deposition gave rise to a whole elimination of SWNTs from the anode. Figure 6 shows 2-dimensional and 3-dimensional tapping mode AFM images of the SWNT film electrophoretically deposited at 150 V for 10 min and its height profile. These images showing densely deposited SWNTs are analogous to the AFM topographies. For the surface with densified structures or with tall structures (usually > 200 nm), the needle-like images as shown in Figure 6 can be easily observed in tapping-mode or non-contact mode AFM.

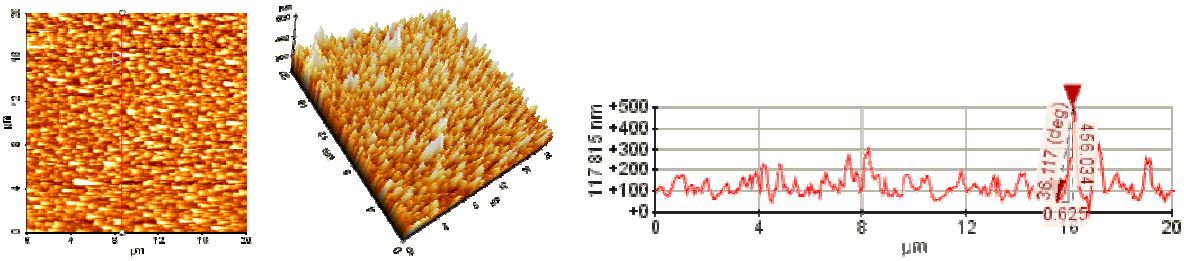

Figure 6. 2-dimensional and 3-dimensional tapping mode images of the SWNT film deposited at 150 V for 10 min using electrophoretic deposition and its height profile.

Figure 7(A) shows a low resolution SEM image of the SWNT film electrophoretically deposited on NH_2 group-terminated gold cathode. The SWNT film was quite uniform in the whole area influenced by the electric field. Figure 7(B) is a magnified image of Figure 7(A) that clearly shows densely-deposited SWNTs on the substrate. The morphology of the SWNT film

was much different from AFM topography of the film in Figure 6. After the electrophoretic deposition of SWNTs was completed, the film-formed cathode was immersed in HPLC DMF, followed by sonication with a different time. Figure 7(C) shows densely packed, vertically aligned SWNT bundles obtained after sonicating the cathode-immersed DMF solution for 2 min. The average diameter of SWNTs in a bundle was about 35 nm which is well agreed with the diameter of SWNTs after being shortened. From this image, it is strongly suggested that densely deposited SWNT bundles are aligned in the vertical direction of the electrode with the assistance of a sonication. The sonication time is an important factor to affect the alignment of SWNTs. The bulky SWNT bundles, shown in Figure 7(C), were partially stripped off from the electrode after 3 min sonication as shown in Figure 7(D). The smaller size of SWNT bundles, with the diameter of ~ 10 nm, remained on the electrode. Some of the SWNTs are lying on electrode due to the decrease in the packing density of SWNTs but mostly still standing. The relatively smaller size of SWNTs, compared to the 3 min sonicated SWNT film, remained much sparsely on electrode by further sonication for 5 min as shown in Figure 7(E).

The attenuated total reflectance (ATR) spectra of electrophoretically deposited SWNT film (a) without sonication and (b) with sonication for 5 min are shown in Figure 7. The sharp peak around 1500 cm^{-1} corresponded to the stretch mode of the aromatic carbon-carbon bond was dramatically reduced after sonication. The amide band around 1600 cm^{-1}, however, was not reduced visibly compared to the C-C stretching peak at 1500 cm^{-1}. That is, due to a strong electric field, many of SWNTs were physically adsorbed onto the SWNTs which were chemically adsorbed at the beginning of applying a dc field.

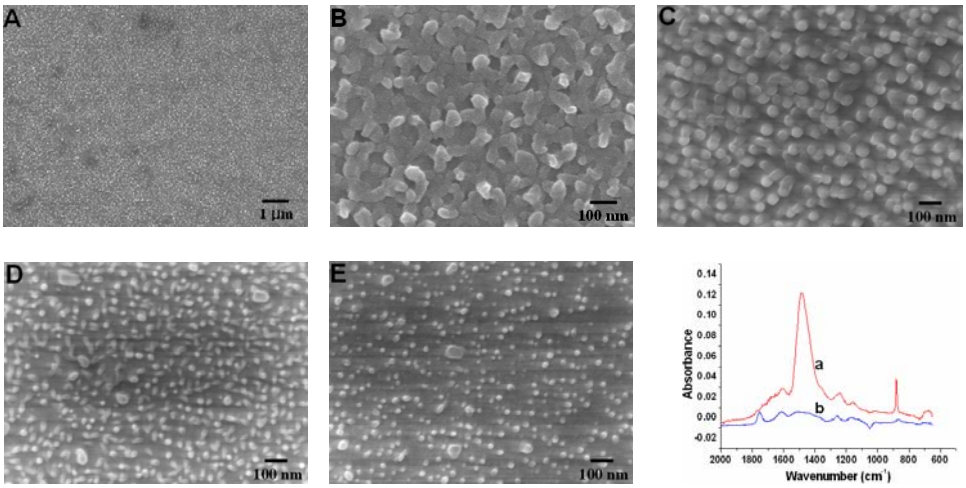

Figure 7. Scanning electron micrographs of SWNT films formed on NH_2-functrionalized gold electrode by applying an electric field at 150 V for 10 min. (A) electrophoretically deposited SWNT film. (B) The magnified image of the SWNT film shown in (A). And the SWNT films sonicated (C) for 2 min, (D) for 3 min and (E) for 5 min in HPLC dimethyl formamide after electrophoretic deposition. Attenuated total reflectance spectra (SENSIR IlluminatIR spectrometer) of the SWNT film (a) without ultrasonic irradiation and (b) with ultrasonic irradiation for 5 min. Band around 1500 cm^{-1} corresponds to the stretch mode of the aromatic carbon-carbon bond. Band around 1600 cm^{-1} corresponds to amide bond.

Figure 8(a) shows the change of surface density and diameter of attached CNTs, which were deposited on gold substrate by applying DC voltage of 150 V, depending on the ultra sonication treatment times. When the sample was treated by 3 min of ultrasonication, CNTs shown a maximum surface density and the average diameter of CNTs were 27 nm. The field emission characteristics of vertically aligned CNTs films as deposited by electrophoretic deposition method, without post treatment of ultra sonication, were shown in Figure 8(b). They showed good field emission properties such as low turn on field and high current density as good as vertically aligned CNTs directly grown on substrate using CVD method. The field emission characteristics of vertically aligned CNTs depending on the ultra sonication treatment will be studied in next 3rd year. Figure 4(c) shows Raman graphs of vertically aligned CNTs depending on the change of Laser polarizing angles.

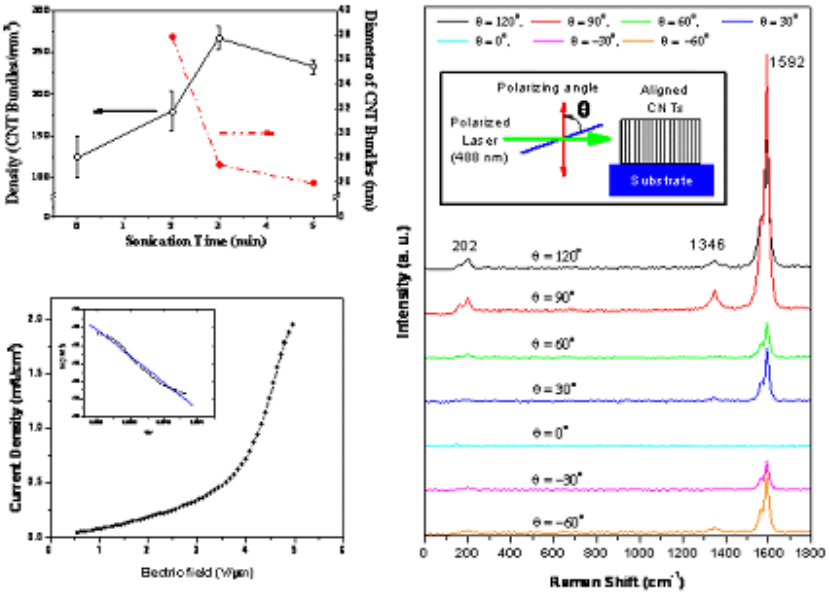

Figure 8. various analysis graphs of vertically aligned CNTs films deposited on gold substrate using electrophoretic deposition method by applying DC voltage of 150 V for 10 min. (a) density and average diameters of vertically aligned CNTs depending on ultrasonication times, (b) Field emission characteristics of CNTs without ultra sonication treatment, (c) Raman graphs of vertically aligned CNTs, after 3min ultra sonication treatment, depending on the change of Laser polarizing angles

Figure 9 shows in detail Figure 7(D), which is magnified from low resolution. The uniform SWNT film in Figure 9 was electrodeposited on the cathode at a DC voltage of 150 V for 10 min and then ultrasonicated for 3 min. The SWNT bundles were well distributed with uniform space between the bundles and mostly aligned in the direction normal to the surface. The arrows in Figure 9(b) indicate the three-bundles-folding structures that can be observed only in standing structures.

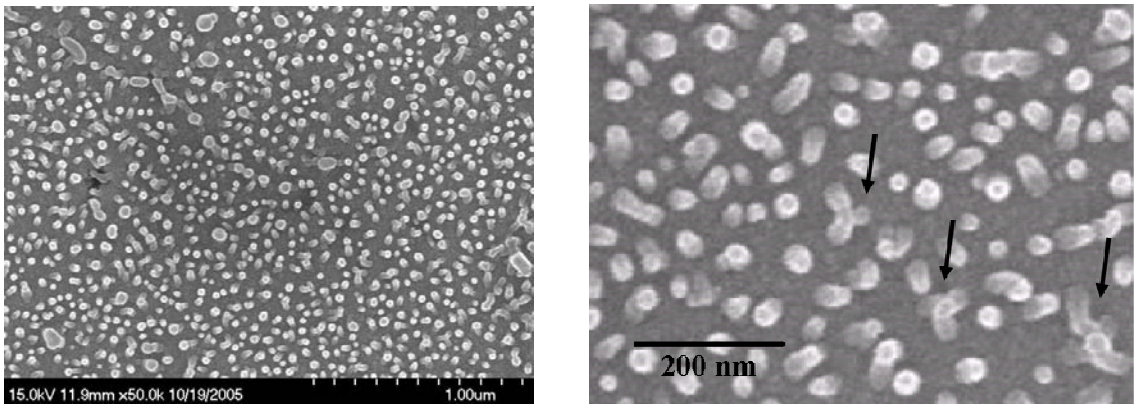

(a) (b)

Figure 9. (a) Scanning electron micrographs of a SWNT film after ultrasonication for 3 min. The film was formed on a gold electrode by applying an electric field at 150 V for 10 min. (b) the magnified image of Figure 9(a). (The arrows indicate the three-bundles-folding structures)

Patterning of SWNT films formed by electrodeposition was performed to control density of the SWNT film by using nanosphere lithography. Scheme 3 shows the schematic for forming the patterns of CNTs via nanosphere lithography on the surface modified with cysteamine by applying electrodeposition to a CNT suspension. The vertical alignment of longer CNTs is difficult to fabricate on plates due to their flexibility. Nanosphere lithography has been thought as a great tool to fabricate a periodic pattern of a nanostructure. Si nanosphere was arrayed into a monolayer on gold substrate using dropping method as shown in Figure 10(a). CNTs would be selectively attached in the holes between nanospheres and form chemical bonding with functionalized substrates. The idea is distinctly promising because nanosphere lithography is greatly effective process to fabricate periodic nanostructure. Figure 10 shows real SEM images of experimental results of the schematic shown in Scheme 3. At first, the Si nanosphere was self-assembled by a simple dropping method, which shown in Figure 10(a). Following the formation of a nanosphere array, SWNT films were electrodeposited on the whole areas both of the surface of nanosphere arrays and the functionalized substrate, which is in the holes between nanospheres. Figure 10(c) shows a hexagonally arrayed CNT patterns with vertical alignment after removing nanospheres by ultrasonic treatment. Field emission analysis will be performed in next 3rd year.

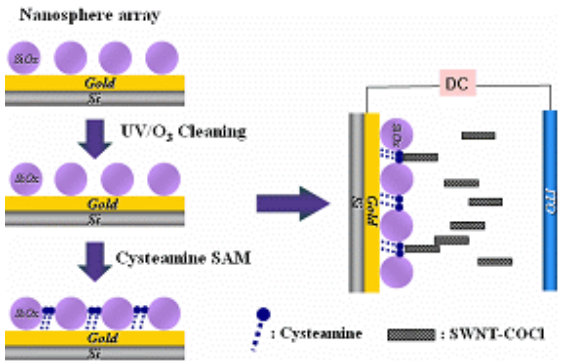

Scheme 3. Schematic for patterning CNT films via nanosphere lithography on the surface modified with cysteamine SAM using electrodeposition.

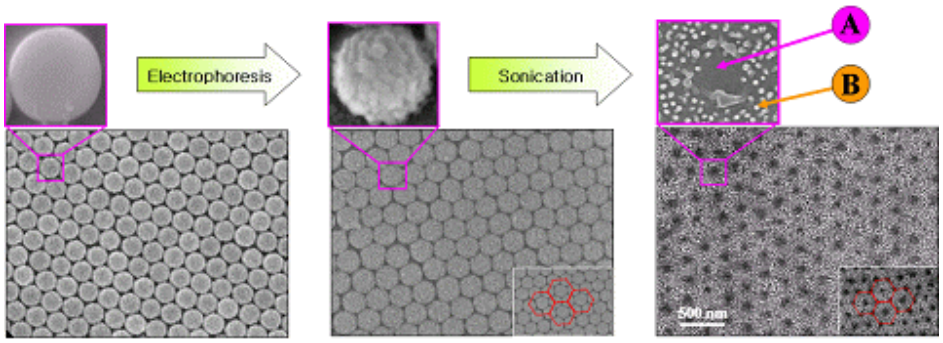

Figure 10. SEM images of experimental results of the schematic shown in Figure 5. (a) Self assembled nanosphere monolayer arrays on substrate, (b) CNT attached Nanosphere arrays after Electrophoresis, (c) uniformly arranged CNTs arrays after removing Nanosphere monolayer by ultra sonication treatment

3. Summary

Carbon nanotubes (CNTs) were functionalized with carboxyl, acid chloride and thiol groups. After the attachments of the functionalized CNTs, the difference in reactivity of functionalized SWNTs was confirmed on the surfaces covered with self-assembled monolayers. Additionally, we have demonstrated selective attachments of chemically functionalized CNTs on modified templates by using AFM and nanosphere lithography, which may contribute to develop the fabrication of 3-D nanostructures on various substrates. Our results of optical trapping drew individual CNT bundles to be manipulated multi-dimensionally, which has a potential application in the fabrication of nanoelectronic devices based on CNTs. A novel and simple method for fabricating the aligned and patterned SWNT film was introduced by using electrodeposition. Ultrasonic treatment after electrodeposition enables randomly deposited SWNT bundles to be aligned normal to the electrode, with appropriate distribution on large areas. Considering that most researchers studying the fabrication of carbon nanotube-based electron emission devices have made great efforts to align carbon nanotubes normal to the electrodes, our method for aligning SWNTs is remarkable in its simplicity. Although it has long been believed that vertically aligned carbon nanotubes were sometimes attributed to ultrasonic treatments, we demonstrated it directly. To pattern SWNT films, nanosphere lithography (NSL) was applied to a SWNT suspension using electrodeposition. The SWNT film was successfully patterned into a hexagonal array, which may contribute to the integration of SWNTs as electron emission sources in electronic devices.

4. Publications

[1] “Multi-dimensional Manipulation of Carbon Nanotubes with Optical Tweezers”, Jianlong Zhang, Hyun Ik Kim, Xiudong Sun, Cha Hwan Oh, Haiwon Lee, Appl. Phys. Lett., 88 (2006) 053123
[2] “Selective Attachment of Functionalized Carbon Nanotubes on Templates Fabricated by AFM and Nanosphere Lithography”, Sung-Kyoung Kim, Ha-Jin Lee, Sun Young Koo, Moon Hee Lee, Haiwon Lee, Mol. Cryst. Liq. Cryst. (accepted)
[3] “Optical Trapping Carbon Nanotubes”, Jianlong Zhang, Hyun Ik Kim, Xiudong Sun, Cha Hwan Oh, Haiwon Lee, Colloids and Surfaces A (accepted)
[4] “Characteristics of Electrodeposited Single-Walled Carbon Nanotube Film”, Sung-Kyoung Kim, Hee-Young Choi, Ha-Jin Lee, Haiwon Lee, J. Nanosci. Nanotech. (accepted)

Multidimensional manipulation of carbon nanotube bundles with optical tweezers

Jianlong Zhang
Department of Physics, Harbin Institute of Technology, Harbin, 150001, People's Republic of China and Department of Chemistry, Hanyang University, Seoul 133-791, Korea

Hyun Ik Kim and Cha Hwan Oh
Department of Physics, Hanyang University, Seoul 133-791, Korea

Xiudong Sun
Department of Physics, Harbin Institute of Technology, Harbin, 150001, People's Republic of China

Haiwon Lee[a)]
Department of Chemistry, Hanyang University, Seoul 133-791, Korea

(Received 21 June 2005; accepted 15 December 2005; published online 3 February 2006)

Optical manipulation of carbon nanotubes (CNTs) in aqueous solution was performed using a linearly polarized infrared tweezers system. Vertical and horizontal manipulation of single-walled and multiwalled carbon nanotubes (SWNTs, MWNTs) was carried out by changing the size of the CNTs and the trapping position. Rotation of MWNT bundles was confirmed using a circular polarized infrared optical tweezers system. Patterning of dots and letters with CNTs was successfully carried out on glass substrates. © *2006 American Institute of Physics*.
[DOI: 10.1063/1.2172020]

Single-walled carbon nanotubes (SWNTs) have received a lot of attention from scientists for their unique chemical and physical properties for use in future nanoelectronics.[1,2] However, because of difficulties in manipulating and sorting individual SWNTs, no remarkable breakthroughs have been made in recent years. General approaches to align carbon nanotubes (CNTs) are either *in situ* or postgrowth. Applied electric fields during the growth of CNTs (Ref. 3) can cause them to align. Several postgrowth alignment methods have been attempted: using an AFM tip,[4] aligning CNTs in solution by applying an electric field[5] or a magnetic field,[6] aligning SWNTs by blending them with liquid crystal,[7] assembling SWNT films by Langmuir-Blodgett methods,[8] and chemical assembly of SWNTs on a large substrate.[9] Although these methods provide a good way to control both the location and orientation of CNTs, they cannot process and sort individual CNTs simultaneously. Optical tweezers[10] is a powerful tool for processing nanosize objects, and this technique can also be used to trap and manipulate SWNTs.[11,12] But in previous reports, only trapping of the CNTs with optical tweezers was given, and manipulation of SWNT bundles vertically and spinning MWNTs vertically have not yet been reported. In order to construct 2D or 3D nanostructures, more exact control of the trapping is essential. In order to explore how to trap and manipulate CNTs more precisely, an infrared optical tweezers system is used to manipulate various CNTs of different fabrication methods, chemical modifications, and sizes.

In this letter, a linearly polarized laser diode (SDL-5432H1, $\lambda = 834$ nm) is used as the trapping light source. The beam expander is composed of two convex lenses. The 120 mW laser beam is strongly focused by an objective lens (Zeith, 100×, oil immersion type, N.A.=1.25, the radius of its back aperture: 2.5 mm) and forms a single-beam optical trap with a diameter less than 1 μm. The sample stage is maintained with a computer-controlled motorized controller (Newport, M-UTM25PP.1, resolution 0.1 μm). The trapping process can be recorded with a CCD camera from linear or circular polarization. A chamber composed of cover- and slide-glass is used to seal a drop of the CNT aqueous solution.

Naturally the short CNT (SWNT and MWNT) bundles have lengths of a few hundred nanometers to 1 μm and diameters of about 20 nm after being cut in mixed acid.[13] All the CNTs used in this study are referred to as CNT bundle, which consist of many short CNTs held together by molecular forces. Figures 1(a) and 1(b) show that one CNT bundle can be trapped vertically and horizontally, respectively. In vertical trapping, the CNT bundle is aligned along the propagation direction of the laser beam while the CNT bundle is aligned along the transverse direction of the laser beam in horizontal trapping. The vertically and horizontally trapped CNTs can be manipulated into any specific position with the optical trap. Vertical trapping was confirmed by a point image because the CCD camera captured top view images. Shorter CNTs are much easier to trap vertically if the focused laser beam is applied to the end of the CNT. Optical tweezers cannot easily trap longer CNTs vertically. If the length of the CNTs is shorter than 10 μm, they can be trapped vertically by decreasing the distance between the substrate and the trapped position just after picking one end. If the distance between the substrate and the trapped position is increased, vertical trapping cannot be achieved. In other words, horizontal trapping of one CNT bundle can be switched to vertical trapping by adjusting the trapping depth (the distance between the cover glass and the trapping position). In our experiment, an oil immersion lens was used to focus the beam. When the trapping depth is zero, the laser intensity is concentrated near the beam focus symmetrically, where the

[a)]Author to whom correspondence should be addressed; electronic mail: haiwon@hanyang.ac.kr

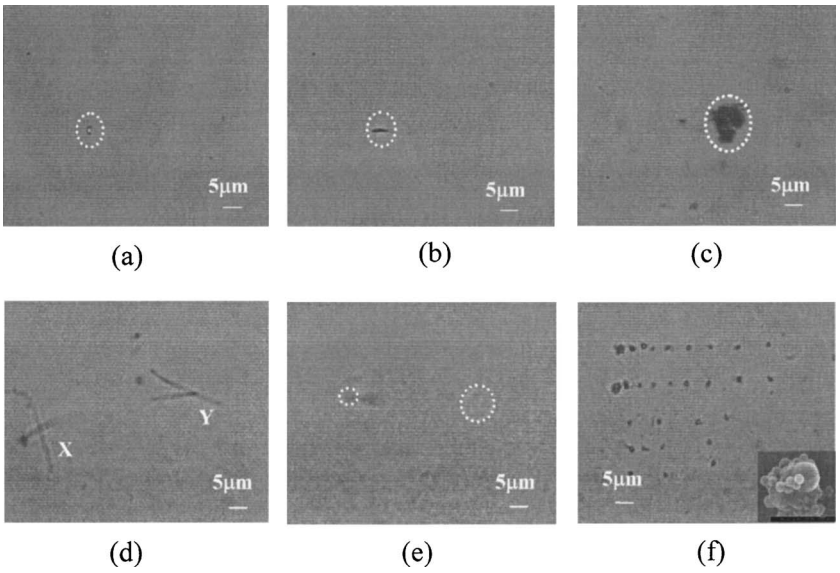

FIG. 1. CCD images of optical manipulation of the CNT bundle: (a) Vertical trapping, (b) horizontal trapping, (c) collective trapping of CNTs in highly concentrated CNT solution, (d) constructing CNT letters horizontally, (e) vertical fixing of a CNT bundle, (f) constructing a CNT/PS array, and inset is a SEM image of one CNT/PS dot.

trapping force would trap a partial position of the CNT bundle but strong enough to hold the whole CNTs. When the trapping depth is increased, the convergence angle decreases and the beam intensity is distributed more along the central axis of the beam before the focus point, which means that the optical trapping force is also distributed along the central axis.[14] This can provide the possibility for long CNTs to be trapped vertically. Small CNT bundles can be trapped collectively as shown in Fig. 1(c). These trapped bundles of CNTs can also be manipulated along the transverse direction by dragging them with the laser beam. Such collective trapping may be due to the induced polarization of originally trapped central CNTs when the dipole moments of the polarized CNTs attract nearby smaller CNTs.[15] The optical trap can manipulate CNTs, so it could also be used to construct special CNTs structures. For example, CNTs could be fixed onto the glass vertically or horizontally. Figure 1(d) shows that by trapping and dragging the CNTs horizontally, two letters were constructed on the glass substrate. Two crossing CNT bundles built the letter "X." The end of one CNT bundle was bound to the side-wall of another CNT bundle to make the letter "Y." Similarly, by manipulating CNTs vertically, bundles can be fixed onto the glass. In Fig. 1(e), one end of the CNTs has been fixed onto the glass marked by a small white circle. The other end of the CNTs is swaying freely in the solution. The position of the optical trap is marked by a big white circle. This manipulation can also be done on ITO glass, which can be used to assemble some CNT-based electronic devices.

Small CNTs with lengths of a few hundred nanometers are rather difficult to fix onto the glass. We fixed the CNTs functionalized with groups of -COCl and PS (polystyrene) particles modified with an amine group together. The mixture was placed at room temperature for 24 h before the trapping experiment, until the ends and sidewalls of most CNTs in the solution were attached to PS particles. Figure 1(f) is a CCD image of a dot array consisting of CNTs and PS particles. The size of the dot was controlled by the application time of the optical tweezers. The large dots on the left of the array were made by a longer application time. The inset SEM image of one dot in Fig. 1(f) shows many PS particles aggregated with CNTs in the optical trap. In this process, the CNTs played an important role as an adhesive to initiate the formation of the large clusters.

MWNTs have been proposed for application in designing nanogears,[16] but how to drive the MWNT gear is an obstacle. Petr Král *et al.* predicted that when MWNTs are irradiated by a circular polarized laser beam, the MWNT bundle can be rotated along its long axis by the angular moment transformation between the laser beam and the nanotubes.[17] Joseph Plewa *et al.* observed the rotation of SWNTs by an optical vortex with a helical pitch.[11] However, the rotation of SWNTs in that report was not the vertical rotation predicted by Petr Král. According to Petr Král's theory, the MWNTs must be trapped vertically first and then can be rotated only by an ordinary laser beam. In our case, this condition can be satisfied. But the trapping position of the MWNTs must be adjusted accurately. If the trapping depth is small and the MWNT bundle is trapped as shown in Fig. 2(a), MWNTs rotate slowly at an angle along the propagation direction of the laser beam, with a rotation frequency of 1 or 2 Hz. The rotation direction follows the polarization direction of the circular polarized laser beam. By increasing the trapping depth, the MWNTs tend to be trapped vertically

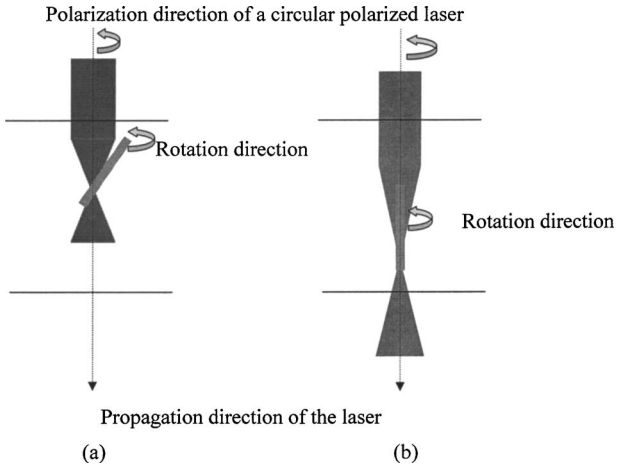

FIG. 2. Rotation of a vertically trapped MWNT bundle in the optical trap: (a) MWNTs rotate slowly along the propagation direction of the laser beam at a certain angle when the trapping depth is small, (b) MWNTs span along its long axis at a high frequency of rotation at a large trapping depth.

completely as shown in Fig. 2(b). In this process, the MWNTs accelerated their rotation frequency until it spun by its long axis, which is much lower than the laser beam frequency due to many factors such as viscous drag in the solution and the large size of the bundle assembly of several individual carbon nanotubes. This result strongly suggests that a focused laser beam can be a driving power for the MWNT motor.

The optical trap can pick up some CNTs selectively, which strongly supports that only semiconductor CNTs in solution could be trapped as reported elsewhere.[12] We also found that the trapping threshold of the laser power depends on the size of the CNT bundle. For CNTs about 5 μm long, the threshold value of the laser beam was 0.4 mW, but the value for the shorter CNT bundle with a length of about 3 μm was 10.5 mW. The threshold value can be defined as the value below which the trapped CNTs would start escaping from the trap. Our measured threshold value is much lower than that of 100 mW reported elsewhere.[12] One reason is due to the small sizes of CNTs used in that work. The other reason is that fluorescence spectroscopy was used to monitor the trapping process which requires a sufficient number of CNTs to be trapped, requiring a high laser power.[12]

Optical trapping can be attributed to the interaction of the electric field component ($\mathbf{E}$) of the trapping laser and the instantaneous dipole moments ($\mathbf{P}$) induced in the SWNTs.[18] The induced dipole moment per unit volume is $\mathbf{P}=\alpha\mathbf{E}$, where α is the first-order polarizability tensor. The interaction energy can be written as

$$\mathbf{U} = -\langle \mathbf{P}\cdot\mathbf{E}\rangle/2 = -\alpha\langle \mathbf{E}\rangle^2/2.$$

The optical force is the negative gradient of the time-averaged potential energy $\mathbf{U}$. The force is determined by the dielectric susceptibility and the gradient of the laser intensity, which will push CNTs to the center of the laser beam where the intensity is higher. But the interaction of the CNTs with the laser is not well understood. More work will be done to explore the dependence of the trapping orientation of the CNTs on the polarization of the laser beam and the dependence of the trapping force on the nonlinear effect of the CNTs.

In conclusion, our results clearly showed that optical tweezers work well in manipulating individual CNT bundles multidimensionally, which has a potential application in the fabrication of 2D or 3D nanoelectronic devices based on CNTs.

This work was supported by Center for Nanostructured Materials Technology and the National Program for Tera-Level Nanodevices as 21st Century Frontier R&D Programs of the Ministry of Science and Technology and also the grant from the AFOSR/AOARD (USA, AOARD-05-4064). The authors also thank Professor Cheol Jin Lee for providing SWNTs and MWNTs.

[1] S. Iijima, Nature (London) **354**, 56 (1994).
[2] P. M. Ajayan and O. Z. Zhou, Top. Appl. Phys. **80**, 391 (2001).
[3] Y. G. Zhang, A. L. Chang, J. Cao, Q. Wang, W. Kim, Y. M. Li, N. Morris, E. Yenilmez, J. Kong, and H. J. Dai, Appl. Phys. Lett. **79**, 3155 (2001).
[4] H. W. C. Postma, A. Sellmeijier, and C. Dekker, Adv. Mater. (Weinheim, Ger.) **12**, 1299 (2002).
[5] X. Q. Chen, T. Saito, H. Yamada, and K. Matsushige, Appl. Phys. Lett. **78**, 3714 (2001).
[6] B. W. Smith, Z. Benes, D. E. Luzzi, J. E. Fischer, D. A. Walters, M. J. Casavant, J. Schmidt, and R. E. Smalley, Appl. Phys. Lett. **77**, 663 (2000).
[7] M. L. Lynch and D. P. Patrick, Nano Lett. **2**, 1197 (2002).
[8] W. H. Zhu, N. Minami, S. Kazaoui, and Y. J. Kim, J. Mater. Chem. **13**, 2196 (2003).
[9] G. R. Saleem, H. Ling, S. Wahyu, and S. H. Hong, Nature (London) **425**, 36 (2004).
[10] A. Ashkin, J. M. Dziedzic, J. E. Bjorkholm, and S. Chu, Opt. Lett. **11**, 288 (1986).
[11] P. Joseph, T. Evan, M. Daniel, and D. G. Grier, Opt. Express **12**, 1978 (2004).
[12] S. D. Tan, H. A. Lopez, C. W. Cai, and Y. G. Zhang, Nano Lett. **4**, 1415 (2004).
[13] J. Liu, A. G. Rinzler, H. J. Dai, R. K. Hafner, P. J. Bradley, A. L. Boul, T. Iverson, K. Shelimov, C. B. Huffman, F. Rodriguez-Macias, Y. Shon, T. R. Lee, D. T. Colbert, and R. E. Smalley, Science **280**, 1253 (1998).
[14] K. B. Im, H. I. Kim, I. J. Joo, C. H. Oh, S. H. Song, P. S. Kim, and B. C. Park, Opt. Commun. **226**, 25 (2003).
[15] D. L. Andrews and D. S. Bradshow, Opt. Lett. **30**, 783 (2005).
[16] D. H. Robertson, B. I. Dunlap, D. W. Brenner, J. W. Mintmire, and C. T. White, Mater. Res. Soc. Symp. Proc. **349**, 283 (1994).
[17] K. Petr and H. R. Sadeghpour, Phys. Rev. B **65**, 161401 (2002).
[18] S. P. Smith, S. R. Bhalotra, A. L. Brody, B. L. Brown, E. K. Boyda, and M. Prentiss, Am. J. Phys. **67**, 26 (1999).

Selective Attachment of Functionalized Carbon Nanotubes on Templates Fabricated by AFM and Nanosphere Lithography

SUNG KYOUNG KIM[1], HA JIN LEE[2], SUN YOUNG KOO[1], MOONHEE LEE[1] and HAIWON LEE[1,*]

[1]Department of Chemistry, Hanyang University, Seoul 133-794, Korea

[2]Materals and Construction Research Division, NIST, Gaithersburg, MD 20899, USA

Abstract

We have investigated a selective attachment of functionalized single-walled carbon nanotubes (SWNTs) on templates. Our efforts have been concentrated on both functionalization of carbon nanotubes and their binding onto templates such as Si-wafer and gold. The alignment of SWNTs was performed by modifying the SWNTs with carboxylic acid, carboxylic chloride and alkyl thiol groups. Functionalized SWNTs were selectively immobilized through the formation of amide bonds using a coupling reagent onto prepatterned nanostructures by a self-assembly method. The characterization of chemically attached carbon nanotubes has been investigated using various surface characterization tools like AFM, TEM, SEM and FT-IR.

Keywords: carbon nanotube, chemical attachment, AFM, nanosphere

Telephone & Fax numbers: +82-2-2220-0945, +82-2-2296-0287

E-mail address: haiwon@hanyang.ac.kr

Introduction

A carbon nanotube has been widely investigated as an essential component for fabrication of nanoelectronic devices and its numerous applications [1]. Especially, well-arrayed carbon nanotubes are highly desired to prepare chemical sensors [2], nanoprobes for scanning probe microscopy [3], field emitter devices [4], etc. Besides their capabilities as functional components, carbon nanotubes are good building blocks for organizing 3-D nanostructure which is another important factor in molecular electronics [5]. In this study, we have investigated a selective attachment of chemically-functionalized single-walled carbon nanotubes (SWNTs) on modified templates by a covalent bonding. If high selectivity of a specific chemical reaction can be controlled, we can design an effective 3-D nanostructure for nano-sized devices using SWNTs as a main frame of the structure. To induce a selective attachment of SWNTs, AFM anodization lithography was engaged in patterning the nanostructures on templates. As another approach to achieving this goal, chemically-modified nanosphere was also used to combine with SWNTs to form the effective nanostructure. Nanosphere lithography has been thought as a great tool to fabricate a periodic array of nanostructure. Therefore, it would be expected to realize the SWNT's nanostructures if the nanosphere is chemically attached to SWNTs.

Experiment

The purified single-walled carbon nanotubes were purchased from Carbon Nanotechnologies Inc. (HiPCO SWNTs), and were used without further purification processes. The $-NH_2$ modified polystyrene (PS)

nanosphere with an average diameter of 190 nm and silicon nanosphere of 400 nm (purchased from Bangs Laboratories, Inc.) were also used as received. The carboxylic acid groups-terminated SWNTs (SWNT-COOH) were prepared by shortening and etching processes using ultrasonification in mixed acids according to the reported procedure [6]. To consider further chemical reaction with chemically modified surface, the carboxylic acid groups on SWNTs were converted into acid chloride groups by treatment with thionylchloride. The acid chloride-functionalized SWNTs (SWNT-COCl) were dispersed in dimethylformamide (DMF) by ultrasonic agitation and were immediately reacted with chemically functionalized surfaces [7]. The formation of functional groups on SWNTs was confirmed by FT-IR [8]. We prepared two kinds of Si surfaces: (i) the surface containing hydroxyl groups (-OH), simply prepared by piranha treatment [9] and (ii) the $-NH_2$ surface by a self-assembly method using 3-(aminopropyl) triethoxymethylsilane [10]. The modified SWNTs were reacted with the two surfaces in DMF suspension of SWNT-COCl for a given time in order to accomplish their chemical attachments. (Scheme 1) After completing the attachment, the reacted substrates were rinsed with deionized water under sonication and were dried under a stream of nitrogen. Non-contact mode atomic force microscopy (XE-100, PSIA Inc.) was exploited to characterize the surface morphologies modified with SWNTs.

Results and Discussion

In the cutting operation of single-walled carbon nanotubes (SWNTs), the 3:1 concentrated H_2SO_4:HNO_3 mixture was used as the oxidizing acid. The shortened nanotubes, having diameters ranging from 700 nm

to 1 μm and lengths from 40 nm to 80 nm, could be produced by ultrasonication in the oxidizing acid at 50 ^{o}C for 6 hr. Figure 1 shows a typical atomic force microscope (AFM) image of the shortened SWNTs which is usually aggregated each other because of van der Waals interaction. SWNTs aggregates are shown including small carbon particles and catalysts as impurities. Cutting time of 6 hr was chosen in order to reduce the most of these impurities such that chemically-functionalized SWNTs could react easily with templates or nanospheres.

Based on chemical reactions of the modified SWNTs with functionalized surfaces, we tried selective attachments of SWNTs on patterned surfaces as shown in Figure 2(a). We chose self- assembled monolayer (SAM) of hexamethyldisilane (HMDS) as a resist whose surface was covered by methyl groups (-CH_3). Since there is no reaction between chemically modified SWNTs and CH_3 groups, SWNT-COCl will be reacted only with the patterned area containing –OH groups. In AFM anodization lithography, patterning was achieved by the growth of silicon oxide which contained –OH groups as shown in Figure 2(b, top). As a result, the patterned area is covered by –OH group while unpatterned area is covered by –CH_3 group. Figure 2(b, bottom) shows selectively attached SWNTs on the protruded SiO_2 region. The height of attached SWNTs on patterned surfaces ranges from 6 nm to 18 nm which are too low for these values to be regarded as those of SWNTs. In fact, the materials attached on line patterns are a kind of carbon which can be clearly confirmed by phase mode AFM. Moreover, in Figure 2(b, bottom), what it was selectively attached means that the chemical reaction occurred only on patterned area. Hence, it can be suggested that line patterns containing –OH groups react rapidly with very thin SWNTs-COCl separated from the

aggregates as well as carbon particles also modified with –COCl since their mobility is better than bulkily-aggregated SWNTs in solution. The similar selective attachment of SWNTs was observed on the various types of patterns.

As another selective attachment of SWNTs, chemical binding of nanospheres-NH_2 with SWNTs-COCl was conducted to fabricate effective nanostructure. Figure 3 shows wonderful images of nanospheres selectively combined with a bunch of SWNTs. In the cutting process of SWNTs using the oxidizing acid, many defects are produced on the side wall of SWNTs, analogous to both ends of SWNTs. These defects also are terminated with –COOH groups which can be active sites to react with substitutes. To date, it has been focused on improving physical, chemical and electrical properties of SWNTs through chemical attachments of useful substances on the side defects of SWNTs from many research groups. The alignment of carbon nanotubes also has been critical issue to apply them to the area of molecular electronics, field emission display, etc. As shown in Figure 3, the PS nanospheres attached on the SWNTs would not seem to change much the properties of SWNTs and also to improve the alignment greatly. However, it is very important to selectively attach nanospheres onto SWNTs because these basic structures have quite a possibility to be used to make a practical application of SWNTs.

Figure 4 shows us an important example for SWNTs to be able to form the 3-D nanostructure in combination with nanospheres. 400 nm of Si nanospheres with no functional group were arrayed as a monolayer on gold substrate as shown in Figure 4(a). Then, SWNTs-COOH were chemically attached to -NH_2 modified gold substrate which was exposed only in the gap between Si nanospheres. In Figure 4(b),

one end of the shortened SWNT is leaning against Si nanosphere due to an intrinsic flexibility of carbon nanotubes and the other end of that is being clearly attached to the gold substrate. This means that the SWNT is standing vertically such that the 3-D nanostructure is formed by using both nanospheres and SWNTs. These results demonstrate critically that the chemical attachments can be used easily to succeed in fabricating the nanostructures.

Conclusion

In conclusion, we have demonstrated selective attachments of chemically functionalized SWNTs on modified templates by using AFM and nanosphere lithography. This work will contribute to develop the fabrication of 3-D nanostructures on various substrates. Furthermore, it enables us to develop nanotube-based electronic devices.

Acknowledgments

This work was supported by 'Center for Nanostructured Materials Technology' under '21st Century Frontier R&D Programs' and the National Program for Tera-Level Nanodevices of the Ministry of Science and Technology as one of the 21century Frontier Programs and also the grant from the AFOSR/AOARD (USA,AOARD-05-4064).

References

[1] Baughman, R.H., Zakhidov, A.A., De Heer, W.A.Collins *Science*, 297, 787, (2002).

[2] Kong, J., Franklin, N.R., Zhou, C.W., Chapline, M.G., Peng, S., Cho, K., Dai, H. *Science*, *287*, 622, (2000).

[3] Wong, S.S., Joselevich, E., Woolley, A.T., Cheung, C.L., Lieber, C.M. *Nature*, *304*, 52, (1998).

[4] Rinzler, A. G., Hafner, J. H., Nikolaev, P., Lou, L., Kim, S. G., Tománek, D., Nordlander, P., Colbert, D. T., Smalley, R. E. *Science*, 269, 1550, (1995).

[5] Rao, C. N. R. *Chemistry of Advanced Materials.* Blackwell Scientific Pub.: Massachusetts, (1993).

[6] Liu, J., Rinzler, A. G., Dai, H., Hafner, J. H., Bradley, R. K., Boul, P. J., Lu, A., Iverson, T., Shelimov, K., Huffman, C. B., Rodriguez-Macias, F., Shon, Y.-S., Lee, T. R., Colbert, D. T., Smalley, R. E. *Science*, 280, 1253, (1998).

[7] Heiney, P. A.., Bruneberg, K., Fang, J. *Langmuir*, 16, 2651, (2000).

[8] FT-IR data (Bruker IFS48, KBr Pellet): 1720 cm^{-1} ($\nu_{C=O}$, SWNT-COOH) and 1770 cm^{-1} ($\nu_{C=O}$, SWNT-COCl).

[9] Ulman, A. *An Introduction to Ultrathin Organic Films from Langmuir-Blodgett to Self-Assembly.* Academic: New York, (1991).

[10] Moon, J.H., Shin, J.W., Kim, S.Y., Park, J.W. *Langmuir*, 12, 4621, (1996).

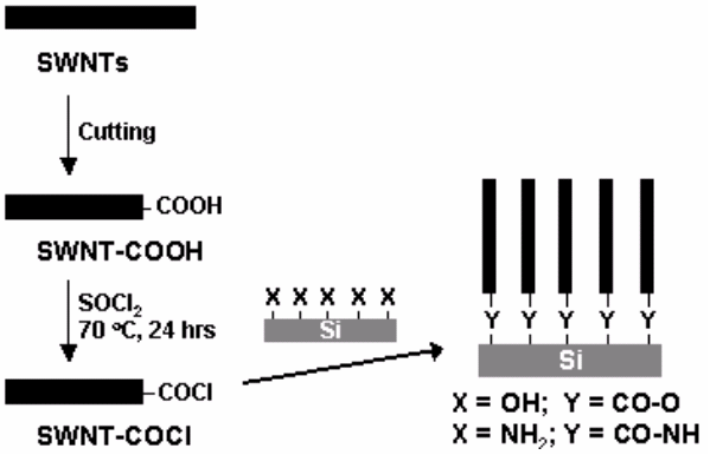

Scheme 1 Schematic view of chemical attachments of SWNTs on modified template.

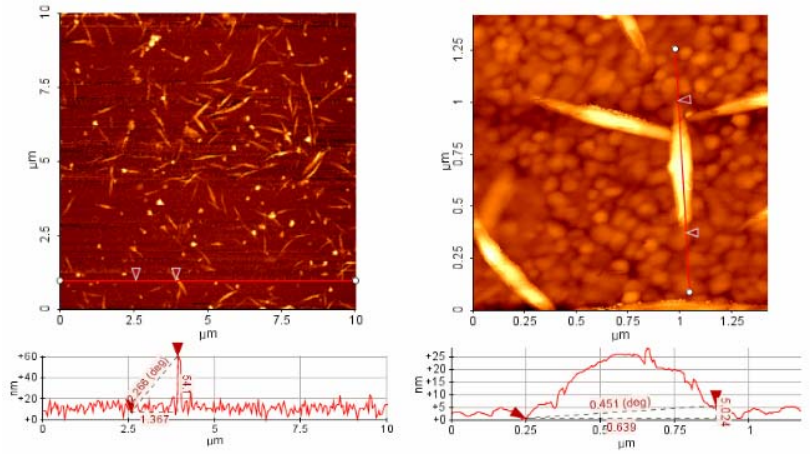

(a) (b)

Figure 1 Typical AFM images of the shortened SWNTs (a) in large area and (b) in small area and their profiles for (a) diameter and (b) length of representative SWNTs.

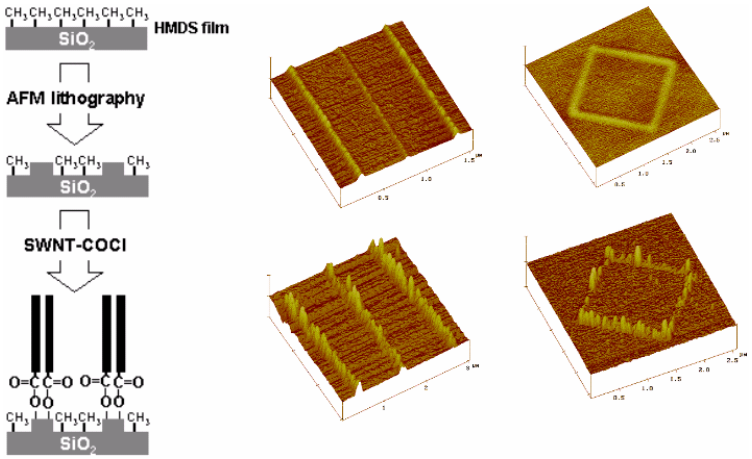

(a) (b)

Figure 2 (a) Schematic for selectively attachments of SWNTs on prepatterned surfaces, representative tapping mode AFM images of patterned HAMD SAM (b, top) before and (b, bottom) after reaction with SWNTs.

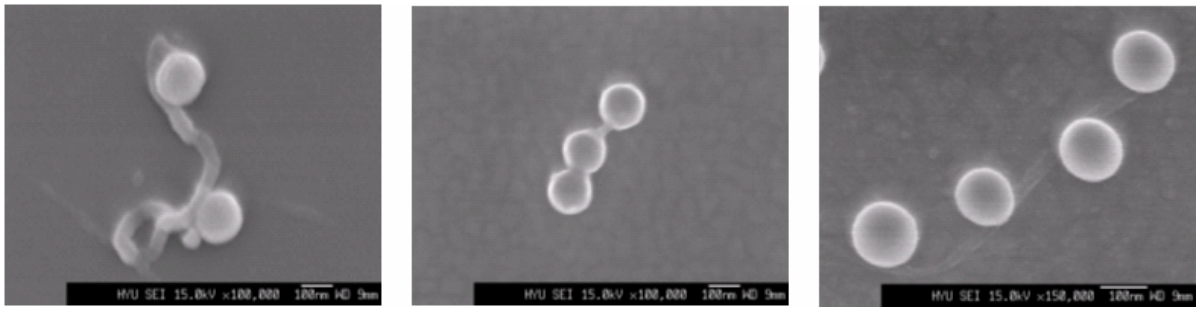

Figure 3 Scanning Electron Microscope (SEM) images of 190 nm of PS nanospheres chemically attached on the SWNTs.

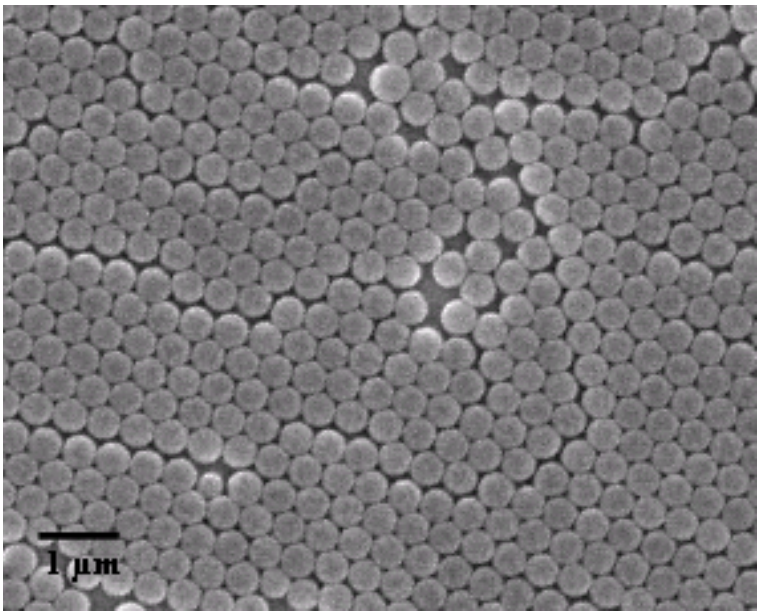

(a)

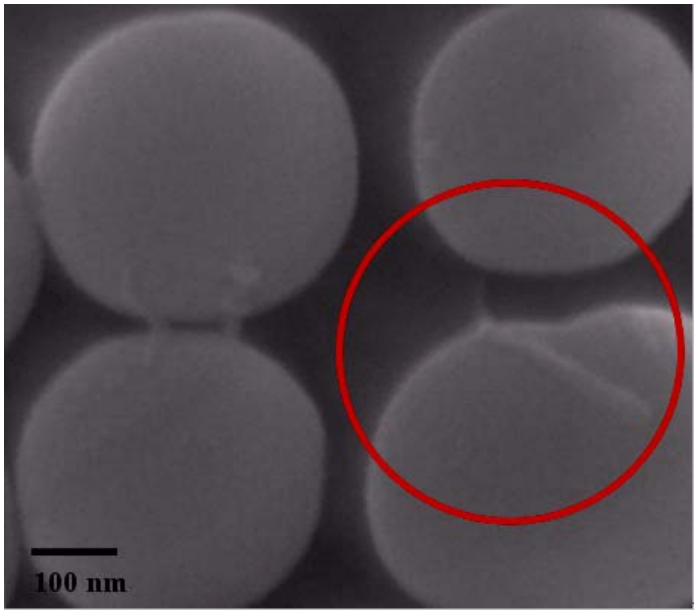

(b)

Figure 4 SEM images of (a) the array of Si nanospheres on gold template and (b) vertically-attached SWNT to gold template using the nanosphere as a supporter.

Available online at www.sciencedirect.com
SCIENCE DIRECT®
ELSEVIER
Colloids and Surfaces A: Physicochem. Eng. Aspects xxx (2005) xxx–xxx
COLLOIDS AND SURFACES A
www.elsevier.com/locate/colsurfa

Optical trapping carbon nanotubes

Jianlong Zhang [a,c], Hyun Ik Kim [b], Xiudong Sun [a], Cha Hwan Oh [b], Haiwon Lee [a,c,*]

[a] *Department of Physics, Harbin Institute of Technology, Harbin 150001, PR China*
[b] *Department of Physics, Hanyang University, Seoul 133-791, South Korea*
[c] *Department of Chemistry, Hanyang University, Seoul 133-791, South Korea*

Received 25 June 2005; received in revised form 26 October 2005; accepted 31 October 2005

Abstract

In this study, multi-dimensional manipulations of CNTs bundles including single- and multi-walled carbon nanotubes (SWNTs and MWNTs) with optical trap are performed. By controlling trapping depth, trapping position and polarization of the laser beam, SWNTs and MWNTs bundles with big sizes can be trapped horizontally or vertically, and the vertically trapped MWNTs can be rotated by optical trap while small CNTs can only be trapped collectively. The CNTs bundles with medium length can be trapped orientated with the polatrization direction of the trapping laser beam. Theoretical calculation based on the interaction between CNTs and laser field shows that the high order nonlinear effect of CNTs in pulsed-laser filed can enhance the trapping force.

Keywords: Carbon nanotubes; Optical trap; Dipole moment

1. Introduction

Since the discovery in 1991 [1], single-walled carbon nanotubes (SWNTs) have attracted a lot of attention worldwide for their unique chemical and physical properties in future nanoelectronics [2]. It is meaningful to align CNTs by applying electrical field or magnetic field in situ or post growth [3–5]. Langmuir–Blodgett [6] or chemical self-assembly [7] also can be used to make anisotropic CNTs film. Using AFM tip is the only way to manipulating individual CNT [8], but AFM tips are too difficult to be integrated for parallel processing. Optical tweezers are powerful for processing nano-size objects [9], including CNTs [10,11]. But in these published reports, only trappings of the CNTs by optical tweezers were given. Manipulation of CNTs bundles vertically and spinning MWNTs were not reported yet. In order to construct two-dimensional or three-dimensional nanostructures, more exact controls of CNTs in the optical trap are essential. In this study, optical trappings of various CNTs including SWNTs and MWNTs synthesized by different methods, functionalized differently and in different sizes were performed and the theoretical discussion was also given based on nonlinear effect of CNTs in the laser field, which was supposed to enhance the trapping force greatly.

2. Experiment

Fig. 1 shows a schematic diagram of the optical tweezers system used in this study. A linearly polarized laser diode (SDL-5432H1, $\lambda = 834$ nm) is used as the trapping light source. The beam expander is composed of two convex lenses. The 120 mW laser beam is focused strongly and forms a single-beam optical trap with the diameter less than 1 μm by an objective lens (Zeith, 100×, oil immersion type, N.A. = 1.25, the radius of its back aperture: 2.5 mm). The sample stage is maintained with a computer-controlled motorized controller (Newport, M-UTM25PP.1, resolution 0.1 μm). Trapping process can be recorded by a CCD camera. Inserting a 1/4-wavelength plate into the light way can perform conversion from linear to circular polarization. A chamber composed of cover- and slide-glass is used to seal a drop of aqueous solution of CNTs. The short CNTs (SWNTs, MWNTs) bundles with the length from a few hundred nanometers to 1 μm and diameter of about 20 nm were prepared as reported [12].

* Corresponding author. Tel.: +82 2 2220 0945; fax: +82 2 2296 0287.
E-mail address: haiwon@hanyang.ac.kr (H. Lee).

0927-7757/$ – see front matter © 2005 Elsevier B.V. All rights reserved.
doi:10.1016/j.colsurfa.2005.10.097

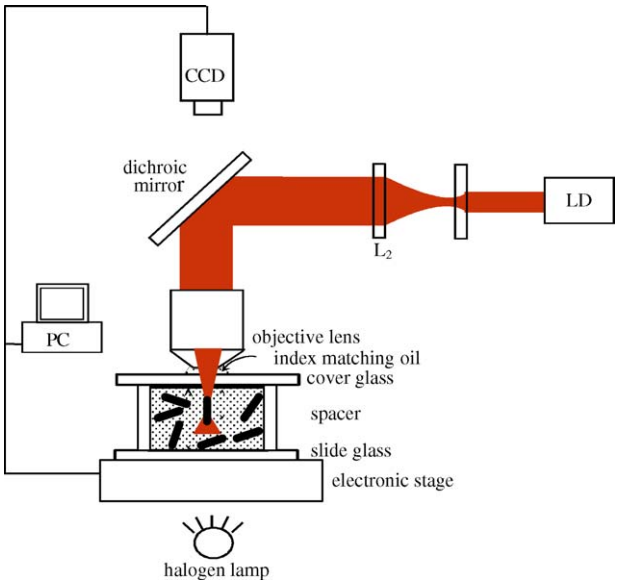

Fig. 1. A schematic diagram of the experiment set-up: LD indicated the laser diode; L_1 and L_2 indicated the convex lenses.

3. Results and discussion

Due to the limited resolution of the CCD camera, CNTs bundles with the length from 3 to 10 μm were chosen for trapping experiments first in order to explore how the orientation of CNTs was controlled in the optical trap. Fig. 2(a) and (b) show that one CNTs bundle could be trapped vertically and horizontally, respectively. In vertical trapping, the CNTs bundle was aligned along the propagation direction of the laser beam while the CNTs bundle was aligned along the transversal direction of the laser beam in horizontal trapping. The vertically and horizontally trapped CNTs could be manipulated to any specific positions by the optical trap. The vertical trapping was confirmed as a point image because the CCD camera captured a top view image. Trapping one end of CNTs and then increasing trapping depth (the distance from cover glass to optical trap) could switch horizontal tapping to vertical trapping. The reason why CNTs bundle can be trapped vertically is due to an oil immersion lens used to tightly focus the laser beam. When the trapping depth is small, the laser intensity is concentrated near the beam focus symmetrically, where the trapping force can only trap a partial position of the CNTs bundle but strong enough to hold the whole CNTs horizontally. When the trapping depth is increased, the convergence angle is decreased and the beam intensity would distribute more along the central axis of the beam before the focus point [13], which means that optical trapping force is also distributed more along the central axis of the laser beam that can provide the possibility for the long CNTs to be trapped vertically along the axial of the trapping beam. This converted trapping is valid for both of SWNTs and MWNTs bundles. But only by converting the laser beam from linear to circular politicization, the vertically trapped MWNTs could be spun by its long axis because of the angular moment transformation between the laser beam and the nanotubes bodies [14].

Used this methodology, we can manipulate CNTs bundles into different shape. Optical trap can capture a CNTs bundle in the chamber and drag it to a specific position. After placing it onto the slide-glass, the optical trap could turn to manipulate the other one. Fig. 3(a) and (b) showed two CNTs bundle were manipulated in parallel and in crossing. Also, the vertically trapped CNTs can be fixed onto the bottom surface of the chamber bottom. In this manipulation experiment, the size of the CNTs was so big that the optical trap only could trap a small part of the whole bundle. The other effect like the polarization induced torque by the laser could be neglected. The trapping force from the intensity gradient of the focused laser beam played a main role in trapping. This optical force competed with the viscous force and Browning movement of the CNTs in the solution. The threshold value of the laser power could be defined as the power below which the CNTs started to escape from the trap. The measured threshold value was ranged from 0.5 to 10 mW depending on the size of the CNTs. This value is lower than that in the report [11]. Fig. 3(c) showed that a CNTs ring was trapped by optical trap. CNTs ring was formed in the cutting process because of self-assembly [15]. The diameter of the CNTs ring was bigger than that of optical trap. But the ring was trapped tightly by the optical trap although it tended to do Browning movement. Even the laser

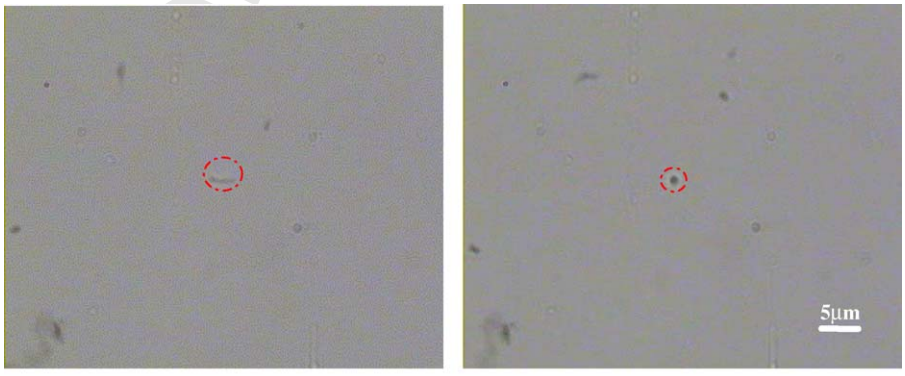

Fig. 2. CCD images of optical manipulating of the CNTs: (a) vertical trapping of a CNTs bundle; (b) horizontal trapping of a CNTs bundle.

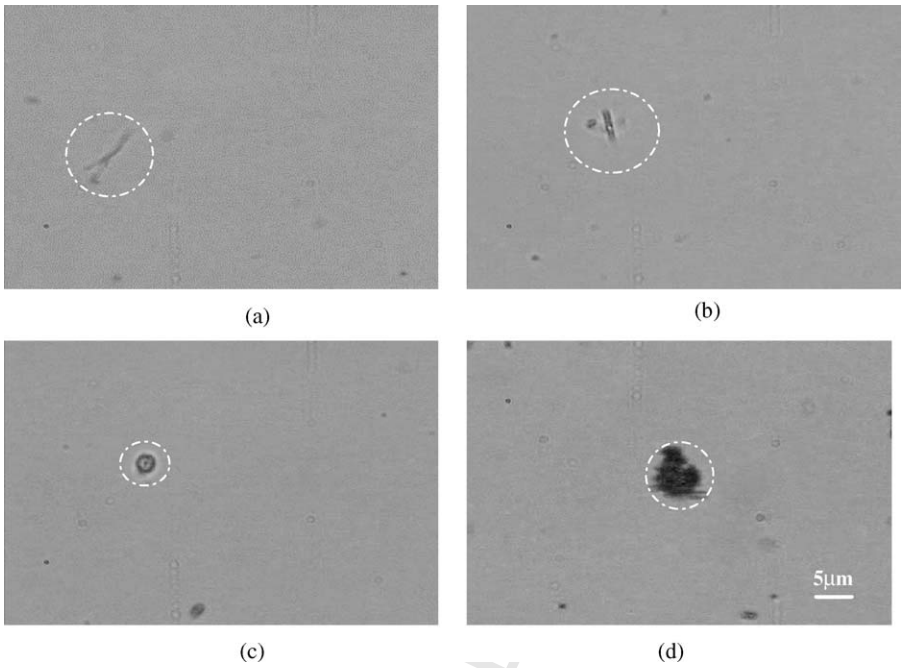

Fig. 3. The manipulation of two long CNTs bundles by optical trap: (a) manipulation of two CNTs bundles in parallel; (b) manipulation of two CNTs bundles in crossing; (c) trapping a CNTs ring; (d) collective trapping of small CNTs bundles.

beam was focused in the hollow area of the ring, the ring was still trapped. If the concentration of the small CNTs was high, optical trap could trap small CNTs collectively as shown in Fig. 3(d). These trapped CNTs could be dragged by optical trap. These collective trapping maybe related to the interaction between the polarized CNTs in the optical trap [16], which can enhance the trapping.

The optical trapping force to CNTs can be attributed to the interaction of the electric field component ($\boldsymbol{E}$) of the trapping laser and the instantaneous dipole moments ($\boldsymbol{P}$) induced in CNTs. The induced dipole moment per unit volume is $\boldsymbol{P} = \alpha \boldsymbol{E}$ [17], where α is the first-order polarizability tensor of CNTs [18]. From this relationship, we can see that for the CNTs with a 1-D molecule with anisomeric character, it is possible to align a CNTs bundle whose orientation is consistent with the polarization of the laser beam. But considering the trapping force is only a few pN, the induced torque to orientate CNTs bundle depends on its length. Fig. 4 gives the dependence of the orientation of the trapped CNTs bundle on its length. For a long CNTs bundle, the torque induced by optical trapping is not high enough to orientate a long CNTs bundle as shown in Fig. 4(a). If the CNTs bundles are too small, for example a few hundred of nanometers, they will be trapped without any orientation in the optical trap as shown in Fig. 3(d). From Fig. 4(b) and (c), we can see this trend.

This equation $\boldsymbol{P} = \alpha \boldsymbol{E}$ is valid when the excited field is weak and only linear polarization is considered. But in the high intensity laser field, such as high-pulsed laser field, the intensity is high enough to induce nonlinear effect in the CNTs, thus the equation could be revised as a nonlinear equation:

$$\boldsymbol{P} = \alpha \boldsymbol{E} + \beta \boldsymbol{E}^2 + \gamma \boldsymbol{E}^3 \quad (1)$$

where the β and γ is second and third nonlinear polarizability tensors. By now, no experiment results about the second order nonlinear optical property of CNTs in the continue wavelength

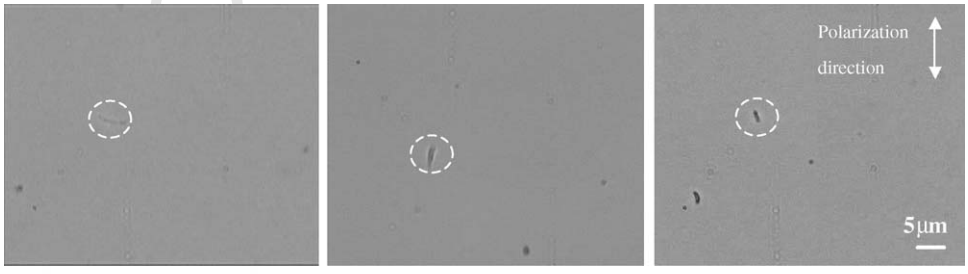

Fig. 4. The orientation of the trapped CNTs bundles depending on the length of CNTs bundles: (a) a random trapping for a long CNTs bundle; (b) trapping of a nicely orientation of a CNTs bundle with the polarization of laser beam; and (c) trapping of a faulty orientation of a short CNTs bundle with the polarization of laser beam. The white arrow indicates the polarization direction of the laser beam.

(CW) laser field were reported. But for the third order nonlinear susceptibility of the SWNTs and MWNTs were investigated theoretically and experimentally in the high short-pulsed laser field [19,20]. If so, the Eq. (1) can be revised into:

$$\boldsymbol{P} = \alpha \boldsymbol{E} + \gamma \boldsymbol{E}^3 \tag{2}$$

Thus, the interaction energy can be written as:

$$U = -\frac{\langle \boldsymbol{P} \cdot \boldsymbol{E} \rangle}{2} = -\left[\frac{\alpha \langle \boldsymbol{E} \rangle^2}{2} + \left(\frac{1}{4}\right)\gamma \langle \boldsymbol{E} \rangle^4\right]$$

$$= -\left[\frac{\alpha \langle \boldsymbol{I} \rangle}{2} + \frac{\gamma \langle \boldsymbol{I} \rangle^2}{4}\right] \tag{3}$$

If only linear term is considered, the optical force is the negative gradient of the time-averaged potential energy U. The force is determined by the dielectric susceptibility and the gradient of the laser intensity. The force in the same direction of the optical intensity gradient will push CNTs to the center of the laser beam where the intensity is high. If the third order nonlinear effect was considered, the trapping force will also depend on the total intensity of the laser beam. It is believed that more new results will be obtained if the optical trapping experiments are done with high-pulsed laser.

4. Conclusion

We reported optical manipulation of SWNTs and MWNTs multi-dimensionally by optical trap in this report. By control trapping depth and CNTs length, one CNTs bundle can be vertical trapped from horizontal trapping by linear polarized optical trap. In horizontal trapping, the orientation of the trapped CNts bundle with the polarization direction of the trapping laser beam depends on the length of the CNTs bundle. Vertical trapped MWNTs bundle can be rotated by circular polarized optical trap due to angular moment transformation between the laser beam and the nanotubes bodies. The trapping force is due to the interaction between the CNTs and the laser field, which is discussed theoretically. The multi-dimensional controls will pave the way to use optical trap to assemble some CNTs based circuit or electronic devices in the future.

Acknowledgements

This work was supported by 'Center for Nanostructured Materials Technology' under '21st Century Frontier R&D Programs' of the Ministry of Science and Technology as one of the 21st century Frontier Programs and also the grant from the AFOSR/AOARD (USA, AOARD-05-4064).

References

[1] S. Iijima, Nature 354 (1994) 56.
[2] P.M. Ajayan, O.Z. Zhou, Top. Appl. Phys. 80 (2001) 391.
[3] Y.G. Zhang, A.L. Chang, J. Cao, Q. Wang, W. Kim, Y.M. Li, N. Morris, E. Yenilmez, J. Kong, H.J. Dai, Appl. Phys. Lett. 79 (2001) 3155.
[4] X.Q. Chen, T. Saito, H. Yamada, K. Matsushige, Appl. Phys. Lett. 78 (2001) 3714.
[5] B.W. Smith, Z. Benes, D.E. Luzzi, J.E. Fischer, D.A. Walters, M.J. Casavant, J. Schmidt, R.E. Smalley, Appl. Phys. Lett. 77 (2000) 663.
[6] W.H. Zhu, N. Minami, S. Kazaoui, Y.J. Kim, J. Mater. Chem. 13 (2003) 2196.
[7] X.L. Nan, Z.N. Gu, Z.F. liu, J. Colloid Interface Sci. 245 (2002) 311.
[8] H.W.C. Postma, A. Sellmeijier, C. Dekker, Adv. Mater. 12 (2002) 1299.
[9] A. Ashkin, J.M. Dziedzic, J.E. Bjorkholm, S. Chu, Opt. Lett. 11 (1986) 288.
[10] P. Joseph, T. Evan, M. Daniel, D.G. Grier, Opt. Exp. 12 (2004) 1978.
[11] S.D. Tan, H.A. Lopez, C.W. Cai, Y.G. Zhang, Nano Lett. 4 (2004) 1415.
[12] J. Liu, A.G. Rinzler, H.J. Dai, R.K. Hafner, P.J. Bradley, A.L. Boul, T. Iverson, K. Shelimov, C.B. Huffman, F. Rodriguez-Macias, Y. Shon, T.R. Lee, D.T. Colbert, R.E. Smalley, Science 280 (1998) 1253.
[13] K.B. Im, H.I. Kim, I.J. Joo, C.H. Oh, S.H. Song, P.S. Kim, B.C. Park, Opt. Commun. 226 (2003) 25.
[14] K. Petr, H.R. Sadeghpour, Phys. Rev. 65 (2002) 161401.
[15] R. Martel, H.R. Shea, Avouris, Nature 398 (1999) 299.
[16] D.L. Andrews, D.S. Bradshow, Opt. Lett. 30 (2005) 783.
[17] S.P. Smith, S.R. Bhalotra, A.L. Brody, B.L. Brown, E.K. Boyda, M. Prentiss, Am. J. Phys. 67 (1999) 26.
[18] X.B. Lorin, G.L. Steven, L.C. Marvin, Phys. Rev. B 52 (1995) 8541.
[19] H.I. Elim, W. Ji, G.H. Ma, K.Y. Lim, C.H. Sow, C.H.A. Huan, Appl. Phys. Lett. 85 (2004) 1799.
[20] Z.W. Wang, C.L. Liu, H. Xiang, Z. Li, Q.H. Gong, Y.J. Qin, Z.X. Guo, D.B. Zhu, J. Phys. D: Appl. Phys. 37 (2004) 1079.

Characteristics of Electrodeposited Single-Walled Carbon Nanotube Film

Sung-Kyoung Kim[a], Hee-Young Choi[a], Ha-Jin Lee[b] and Haiwon Lee[a*]

[a]*Department of Chemistry, Hanyang University, Seoul, 133-791, Korea.*

[b]*Korea Basic Science Institute Jeonju Center, Jeonju, 561-756, Korea.*

[*]Author to whom correspondence should be addressed.
E-mail address: haiwon@hanyang.ac.kr.

Abstract

Thin films of chemically-functionalized single walled carbon nanotubes (SWNTs) were fabricated by using a direct current (DC) electrodeposition method. SWNTs were shortened and then functionalized with acid chloride group to combine with amine group-terminated gold substrate. The electrodeposited SWNT films were characterized by using Raman spectroscopy, attenuated total reflectance infrared (ATR/IR) spectrometry and atomic force microscopy. We demonstrated that the SWNT film was well distributed on an electrode with robust adhesion.

Keywords: single-walled carbon nanotubes, electrodeposition, CNT thin film.

1. INTRODUCTION

Single-walled carbon nanotubes (SWNTs) have been considered as potential candidates for nanoscience and nanotechnology due to their outstanding properties, such as excellent mechanical property, metal-like electrical conductivity and high aspect ratio.[1] Recently, there has been an intense interest in development of thin films of carbon nanotubes on conductive surfaces for the applications as electron emission devices, large surface area electrodes and sensing devices.[2-4] The thin films of carbon nanotube could have been fabricated using various methods, such as chemical vapor deposition (CVD)[5], screen-printing[6], electrodeposition[7], filtration[3], spraying[8], self-assembling[9], etc. We employed the electrodeposition method among them to fabricate thin films of carbon nanotube because there are several advantages in following aspects: its simple set-up, short time in processing, robust adhesion of films, no impurity, easy control of film thickness, etc. Shortly speaking of electrodeposition, carbon nanotubes suspended in a solution are forced to move toward the electrode by applying an electric field to the suspension. The carbon nanotubes collect on one of the electrodes and form a coherent deposit on it. However, the electrodeposition affected by various factors was not explained in detail in each process by now, as well as not characterized well for the products of thin films. Here, we report our observations for the electrodeposition of acid

chloride-functionalized SWNTs dispersed in dimethyl formamide (DMF). The characteristics of electrodeposited SWNT films demonstrated by using various methods, such as Raman spectroscopy, attenuated total reflectance infrared (ATR/IR) spectrometry and atomic force microscopy are also described.

2. EXPERIMENTAL DETAILS

2.1. Preparation of functionalized SWNTs

As-grown single-walled carbon nanotubes (Carbon Nanotechnologies, Inc., HiPCO SWNTs) were treated at elevated temperature and then shortened by well-known process using the oxidizing acid.[12] The shortened nanotubes were purified in a 5 M HCl solution under ultrasonic treatment, resulted in carboxylic acid-functionalized SWNTs. The COOH-SWNTs were further reacted with $SOCl_2$ to convert the carboxylic acid groups into the corresponding acid chloride at 70 ^{o}C. The black COCl-SWNTs suspension was centrifuged repeatedly at 5000 rpm for a few hours to eliminate remaining reactants and sufficiently washed with $CHCl_3$, and then dried in vaccum oven. The COCl-SWNTs were dispersed again in dimethyl formamide (DMF) with the concentration of about 0.3 mg/mL by ultrasonic treatment.

2.2. Electrodeposition of SWNTs

The method of electrodeposition was employed to deposit the acid chloride-functionalized SWNTs on amine-modified gold substrate. In the quartz cell containing the nanotube suspension, the gap distance between the gold substrate as cathode and the bare ITO as anode was fixed at 0.8 cm by the spacer. The direct current (DC) voltage of 150 V or 50 V was applied between the two electrodes for 10 min. If it is not noted particularly, a SWNT film was fabricated at 150 V of a DC field applied for 10 min.

2.3. Characterization of the SWNT film

Attenuated total reflectance infrared (ATR/IR) spectrometry (SensIR IlluminatIR spectrometer) equipped with a liquid nitrogen-cooled MCT detector was used to investigate the quantitative property of the SWNT film. Infrared absorption spectra were collected first on a bare gold plate as a background unit and subsequently on a SWNT film-formed gold plate which is annealed at 70 ^{o}C for 30 min. Surface property measurement of a SWNT film was conducted by a Raman confocal scanning microscope (Nanofinder 30, Tokyo Instruments, Inc.) by exciting with the 488 nm (Sapphire) radiation line. To remove an appreciable peak shift caused by the laser heating, low power of 1 mW was employed on the sample surface with the exposure

time of 10 sec. Using the x, y scan stage, Raman scattered light and 2-D spectral image of a SWNT film were obtained at 1.12 cm^{-1} step intervals in a backscattering geometry using -70 ^{o}C-cooled CCD for the phonon detection.

3. RESULTS AND DISCUSSION

Figure 1 shows single walled carbon nanotubes (SWNTs) before and after shortening process. The acid chloride-functionalized SWNTs (COCl-SWNTs) had no iron catalytic particles generated in the HiPCO process. The length of highly-entangled, raw SWNTs (usually > 10 μm) was reduced to less than 1 μm with a rod-like shape. We found that the crystallinity of SWNTs was conserved even after shortening process using the oxidizing acid as shown in Figure 1(b).

Dimethyl formamide (DMF) has been known as a good solvent in dispersing SWNTs. DMF has the dielectric constant of about 37 at 25 ^{o}C that is high enough to be applied to electrodeposition process. DMF, here, was used as a solvent in the COCl-SWNT suspension without the addition of ionic compounds. SWNTs are a good candidate for an electrodeposition and movable in DMF solution because they are easily charged under an electric field due to the metal-like properties of carbon nanotubes. Figure 2 suggests the electrodeposition process of COCl-SWNT in dimethyl formamide.

When an electric field was applied to the SWNT suspension, the SWNT aggregates were produced immediately in the suspension. The COCl-SWNTs, however, were well dispersed in dimethyl formamide (DMF) before applying an electric field. Since the stability in dispersion usually decreases with increasing ionic concentration, it is suggested that chloride ions are produced by dissociating from acid chloride groups on SWNTs under the influence of DC field.[13] A good leaving group of Cl^- in COCl-SWNT was simply confirmed by adding a small amount of a silver ion to SWNT suspension. While the sediment of AgCl was produced especially near the anode during applying an electric field, the sediment in SWNT suspension was not observed due to the absence of Cl^- ion under no influence of an electric field. In the middle space between two electrodes, the polarized SWNTs under an electric field are stabilized in charge due to the compensation of chloride ions as shown in Figure 2(A: middle space).[14] The SWNTs near both electrodes migrated with a high speed toward the electrodes, caused by a strong charge interaction. On the cathode terminated with amine groups, a uniform SWNT film was formed with a covalent bond as shown in Figure 2(B: cathode). After prolonged deposition time, the coagulated SWNTs were difficult to be deposited on the electrode because of its irregular shape.[15] The dissociated chloride ions, Cl^-, migrate toward the positive electrode. The increase in the concentration of chloride ions near the

anode resulted in the assembly of SWNTs in a bundle as shown in Figure 2(C: anode). The assembly of SWNTs also comes from the strong electric field analogous to the previous report.[14]

The acid chloride-functionalized SWNTs (COCl-SWNTs) were deposited on the NH_2-modified gold substrate by applying a DC field at 150 V or 50 V for 10 min. Figure 3(a) presents the densely deposited, uniform SWNT film obtained at a DC field of 150 V. The formation of a SWNT film in electrodeposition depends on various factors, such as concentration of SWNT, strength of electric field, nature of electrolyte, etc. The thickness of SWNT film was controlled with a variation in the concentration of SWNT, the strength of electric field and the applying time. The aggregation of SWNTs, however, has occurred seriously at higher concentration (> 0.8 mg/ml at 150 V) of SWNTs in DMF, resulting in the SWNT film with low uniformity. The increase in the concentration of a chloride ion on anode made SWNTs aggregated into bundles which were attached on anode with poor adhesion. On the contrary, COCl-SWNTs were deposited robustly on the cathode either of a bare gold or of a gold modified with cysteamine. In addition, the uniform films of SWNTs were obtained on both of the gold cathodes. The adhesion of the films in both cases was strong, but showing a different stablility under the influence of ultrasonication. To investigate adhesion property of the

electrodeposited SWNT film, physisorbed and chemisorbed SWNT films were fabricated at 50 V of an electric field applied for 10 min on a bare gold and on a cysteamine-modified gold, respectively. Then, ultrasonication was applied to both of the films for 3 min. The infrared adsorption spectra in Figure 3(b) were obtained on the samples to investigate the quantity of SWNTs in the films. In this work, the most distinct peak in the spectra of the SWNT films was the absorption band of the stretch mode of the aromatic carbon-carbon bond observed at about 1500 cm^{-1}. Although the peak intensity of the physisorbed SWNT film on a bare gold was similar with that of the chemisorbed SWNT film on a cysteamine-modified gold, the intensity of the physisorbed film was lower than that of the chemisorbed film after ultrasonication for 3 min. The result shows that physically adsorbed COCl-SWNTs on a bare gold are easily detached compared to chemically adsorbed COCl-SWNTs on NH_2-terminated gold under ultrasonication.

To characterize the electrodeposited SWNT film in detail, we introduced tapping-mode atomic force microscope (AFM) in imaging the SWNT film. The results induced needle-like topography from which one can be confused as if SWNTs were vertically aligned on a substrate. The needle-like image comes from the particular scanning system of AFM, by which the AFM tip is vibrated perpendicular to the substrate in

tapping mode or in non-contact mode. The densely packed SWNTs and the big differences in the height of the structure (> ~ 100 nm) also play a key role to present a needle-like topography in AFM image. As an another trial, the distribution of SWNTs in a SWNT film was surveyed by imaging the film using Raman spectroscopy which provides chemical and structural information of a sample. Figure 4(a) shows confocal Raman images (15×15 μm^2) recorded by scanning a SWNT film with the focused laser. The images were acquired by detecting intensity of the RBM mode (172 cm^{-1}), Raman D band (1332 cm^{-1}) and G band (1578 cm^{-1}), respectively, upon laser excitation at 488 nm. From the contrast of the images, it was found that a SWNT film was composed entirely of the SWNTs with defect sites. Figure 4(b) shows the representative Raman scattering spectrum for the SWNT film, which provides typical four main Raman shifts of SWNT: RBM (~100 – 300 cm^{-1}), Raman D band (~1300cm^{-1}), G band (~1592 cm^{-1}), and G' band (~2600 cm^{-1}).[16] The frequency of the RBM is very sensitive to the tube diameter. The isolated tubes are concerned the following equation, $\mathbf{v}$ (cm^{-1}) = $\mathbf{A}/\mathbf{d}$ (nm), where **v** is the RBM frequency, **d** SWNT diameter, **A** proportionality constant. The diameters of the electrodeposited SWNTs (1.2 nm ~ 1.4 nm), however, were well agreed with those of the typical HiPCO SWNTs (0.8 nm ~ 1.4 nm) when applying various relations between the RBM frequency and the inverse of the SWNT diameter.[17-20] The

magnified Raman image at G band (1578 cm^{-1}) of the SWNT film is shown in Figure 3(c), in which the high intensity of Raman G band (showing red and deep yellow colors) could be observed for the SWNTs even after shortening process and subsequent electrodeposition process. The G band originating from the tangential oscillations of the carbon atoms in the nanotube defines ordered carbons with metallic or semiconducting helicity. Therefore, the electrodeposited SWNT films were demonstrated to have the property of electrical conductivity which is very important for the future applications of SWNT films.

4. CONCLUSION

In conclusion, we demonstrated well distributed SWNT films using DC electrodeposition method. The characterization of the SWNT film was performed using Raman spectroscopy, attenuated total reflectance infrared (ATR/IR) spectrometry, atomic force microscopy. As a result, the properties of adhesion and electrical conductivity have drawn the possibility of a SWNT film applied to potential applications like electron emitters and large surface area electrodes. Deep understanding for the electrodeposition of SWNTs would contribute to promoting the properties of a SWNT film such as uniformity, adhesion, density, alignment, etc. The simple

fabrication of a SWNT film using DC electrodeposition would enable SWNTs to be integrated into electronic devices, especially electron emission devices.

Acknowledgment: This work was supported by a grant(code #: 05K1501-01210) from 'Center for Nanostructured Materials Technology' under '21st Century Frontier R&D Programs' of the Ministry of Science and Techonlogy, Korea and also a grant from the AFOSR/AOARD (USA,AOARD-05-4064).

References and Notes

1. R. H. Baughman, A. A. Zakhidov and W. A. de Heer, *Science* 297, 787 **(2002)**.

2. S. J. Oh, J. Zhang, Y. Cheng, H. Shimoda and O. Zhou, *Appl. Phys. Lett.* 84, 3738 **(2004)**.

3. Z. Wu, Z. Chen, X. Du, J. M. Logan, J. Sippel, M. Nikolou, K. Kamaras, J. R. Reynolds, D. B. Tanner, A. F. Hebard and A. G. Rinzler, *Science* 305, 1273 **(2004)**.

4. J. Sippel-Oakley, H. T. Wang, B. S. Kang, Z. Wu, F. Ren, A. G. Rinzler and S. J. Pearton, *Nanotechnology* 16, 2218 **(2005)**.

5. Z. P. Huang, D. L. Carnahan, J. Rybczynski, M. Giersig, M. Sennett, D. Z. Wang, J. G. Wen, K. Kempa and Z. F. Ren, *Appl. Phys. Lett.* 82, 460 **(2003)**.

6. K. Nishimura, Z. Shen, M. Fujikawa, A. Hosono, N. Hashimoto, S. Kawamoto, S. Watanabe and S. Nakata, *J. Vac. Sci. Technol. B* 22, 1377 **(2004)**.

7. Y. Abe, R. Tomuro and M. Sano, *Adv. Mater.* 17, 2192 **(2005)**.

8. C. Bower, O. Zhou, W. Zhu, A. G. Ramirez, G. P. Kochanski and S. Jin, *Mater. Res. Soc. Symp. Proc.* 593, 215 **(2000)**.

9. O. J. Lee, S. H. Jeong and K. H. Lee, *Appl. Phys. A* 76, 599 **(2003)**.

10. Q. Chen and L. Dai, *Appl. Phys. Lett.* 76, 2719 **(2000)**.

11. J. C. Hulteen, D. A. Treichel, M. T. Smith, M. L. Duval, T. R. Jensen and R. P. Van

Duyne, *J. Phys, Chem. B* 103, 3854 **(1999)**.

12. J. Liu, A. G. Rinzler, H. Dai, J. H. Hafner, R. K. Bradley, P. J. Boul, A. Lu, T. Iverson, K. Shelimov, C. B. Huffman, F. Rodriguez-Macias, Y. S. Shon, T. R. Lee, D. T. Colbert and R. E. Smalley, *Science* 280, 1253 **(1998)**.
13. O. O. Van der Biest and L. Vandeperre, *J. Annu. Rev. Mater. Sci.* 29, 327 **(1999)**.
14. P. V. Kamat, K. G. Thomas, S. Barazzouk, G. Girishkumar, K. Vinodgopal and D. Meisel, *J. Am. Chem. Soc.* 126, 10757 **(2004)**.
15. Y. Abe, R. Tomuro and M. Sano, *Adv. Mater.* 17, 2192 **(2005)**.
16. A. Jorio, R. Saito, J. H. Hafner, C. M. Lieber, M. Hunter, T. McClure, G. Dresselhaus and M. S. Dresselhaus, *Phys. Rev. Lett.* 86, 1118 **(2001)**.
17. N. Anderson, A. Hartschuh, S. Cronin and L. Novotny, *J. Am. Chem. Soc.* 127, 2533 **(2005)**.
18. S. Rols, A. Righi and J. L. Sauvajol et al, *Eur. Phys. J.* B 18, 201 **(2000)**.
19. X. Zhang, W. Zhang, L. Liu and Z. X. Shen, *Chem. Phys. Lett.* 372, 497 **(2003)**.
20. A. M. Rao, J. Chen, E. Richter, U. Schlecht, P. C. Eklund, R. C. Haddon, U. D. Venkateswaran, Y. –K. Kwon and D. Tomanek, *Phys. Rev. Lett.* 86, 3895 **(2001)**.

Figure Captions

Fig. 1. Transmission electronic micrographs of a bunch of (a) raw SWNTs and (b) acid chloride-functionalized SWNTs. The insets show each TEM image in a low resolution.

Fig. 2. Schematic view of the electrodeposition process of COCl-SWNTs in dimethyl formamide.

Fig. 3. (a) Scanning electron micrographs of a SWNT film formed on NH_2-functionalized gold electrode by applying an electric field at 150 V for 10 min. (b) Infrared absorption spectra of the SWNT films (A) physisorbed, (B) physisorbed and subsequently ultrasonic-irradiated for 3 min, (C) chemisorbed and (D) chemisorbed and subsequently ultrasonic-irradiated for 3 min. The films were obtained either on a bare gold (physisorption) or on a cysteamine-modified gold (chemisorption) by applying a DC field of 50 V for 10 min. Band around 1500 cm^{-1} corresponds to the stretch mode of the aromatic carbon-carbon bond.

Fig. 4. (a) Raman spectral images of a SWNT film deposited on gold substrate. The contrast in the images presents the local intensity of the RBM mode (172 cm^{-1}), Raman D band (1332 cm^{-1}) and G band (1578 cm^{-1}), (b) Raman scattering spectrum for the SWNT film and (c) the magnified Raman spectral image of the film at Raman G band (1578 cm^{-1})

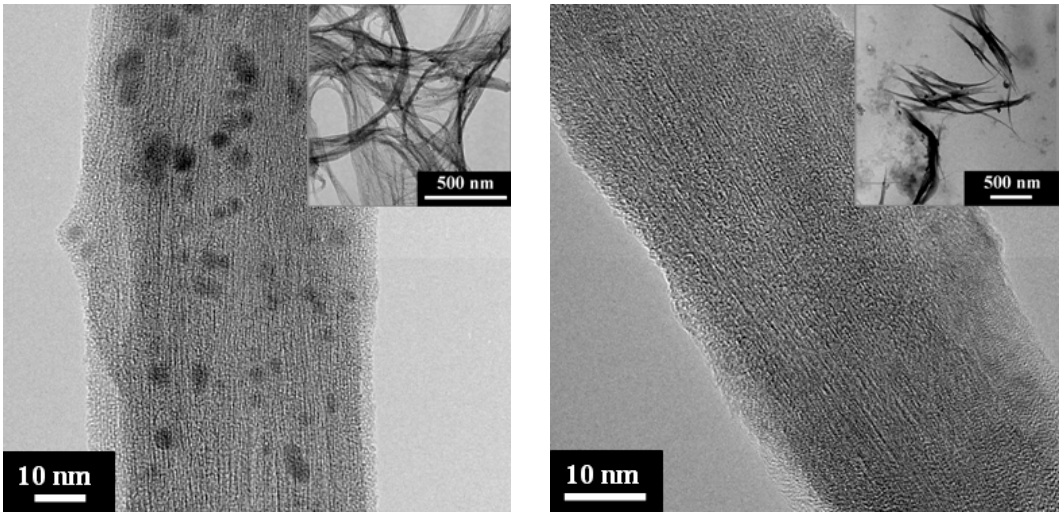

(a) (b)

Fig. 1. Transmission electronic micrographs of a bunch of (a) raw SWNTs and (b) acid chloride-functionalized SWNTs. The insets show each TEM image in a low resolution.

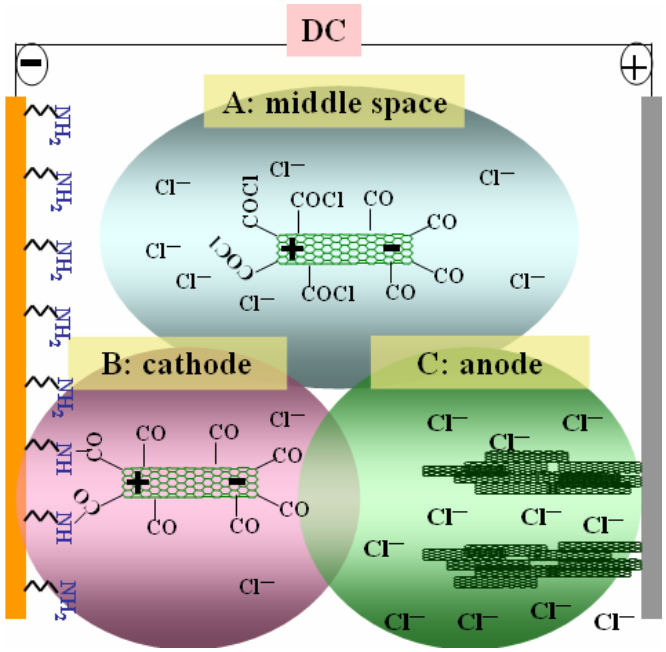

Fig. 2. Schematic view of the electrodeposition of COCl-SWNTs in dimethyl formamide.

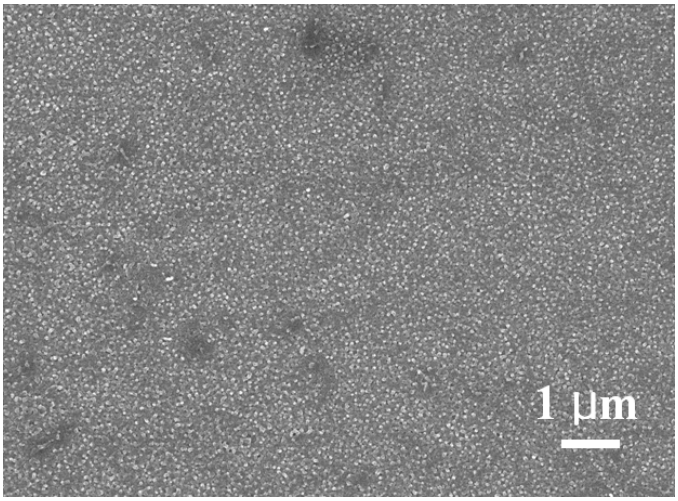

(a)

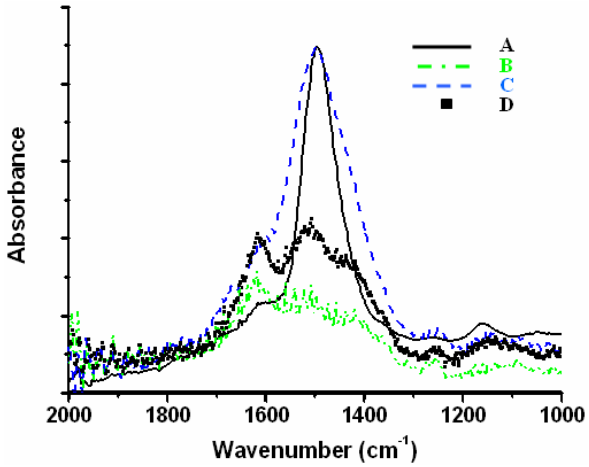

(b)

Fig. 3. (a) Scanning electron micrographs of a SWNT film formed on NH_2-functionalized gold electrode by applying an electric field at 150 V for 10 min. The inset shows a magnified image of the SWNT film. (b) Infrared absorption spectra of the SWNT films (A) physisorbed, (B) physisorbed and subsequently ultrasonic-irradiated for 3 min, (C) chemisorbed and (D) chemisorbed and subsequently ultrasonic-irradiated for 3 min. The films were obtained either on a bare gold (physisorption) or on a cysteamine-modified gold (chemisorption) by applying a DC field of 50 V for 10 min. Band around 1500 cm^{-1} corresponds to the stretch mode of the aromatic carbon-carbon bond.

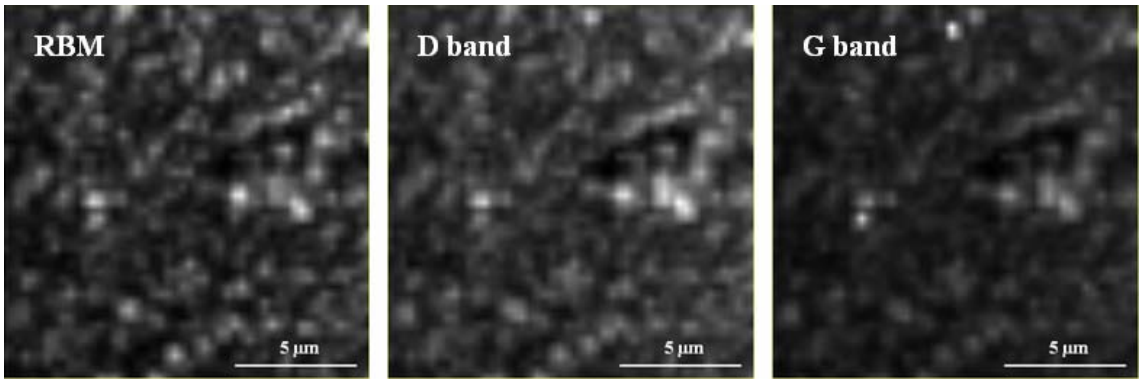

(a)

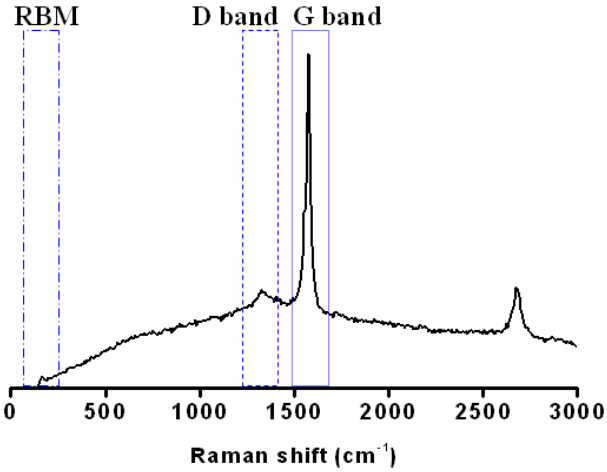

(b)

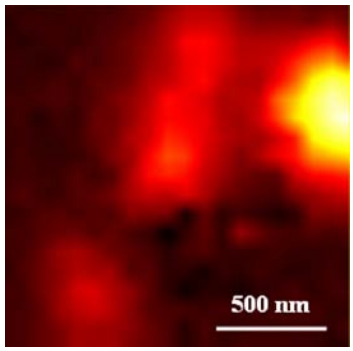

(c)

Fig. 4. (a) Raman spectral images of a SWNT film deposited on gold substrate. The contrast in the images presents the local intensity of the RBM mode (172 cm^{-1}), Raman D band (1332 cm^{-1}) and G band (1578 cm^{-1}), (b) Raman scattering spectrum for the SWNT film and (c) the magnified Raman spectral image of the film at Raman G band (1578 cm^{-1})